

AD-A134 740

INTRACAVITY LASER EXCITATION OF NCO FLUORESCENCE IN AN
ATMOSPHERIC PRESSU. (U) ARMY ARMAMENT RESEARCH AND
DEVELOPMENT CENTER ABERDEEN PROVIN.

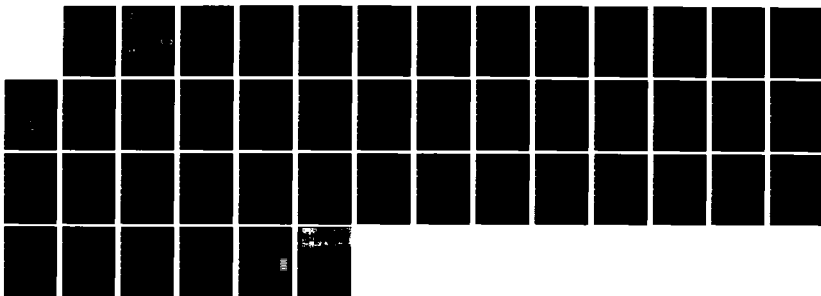
1/1

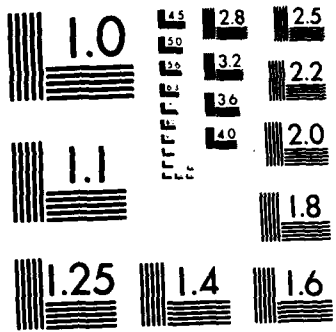
UNCLASSIFIED

W R ANDERSON ET AL. SEP 83 ARBRL-TR-02527

F/G 21/2

NL





MICROCOPY RESOLUTION TEST CHART
NATIONAL BUREAU OF STANDARDS-1963-A

AD-A134740

12

ADF 300 344

TECHNICAL REPORT ARBRL-TR-02527

INTRACAVITY LASER EXCITATION OF N₂O
FLUORESCENCE IN AN ATMOSPHERIC
PRESSURE FLAME

William R. Anderson
John A. Vanderhoff
Anthony J. Kotlar
Mark A. DeWilde
Richard A. Beyer

September 1983

DTIC
ELECTE
NOV 8 1983
S B



US ARMY ARMAMENT RESEARCH AND DEVELOPMENT COMMAND
BALLISTIC RESEARCH LABORATORY
ABERDEEN PROVING GROUND, MARYLAND

Approved for public release; distribution unlimited.

DTIC FILE COPY

83 11 07 057

Destroy this report when it is no longer needed.
Do not return it to the originator.

Additional copies of this report may be obtained
from the National Technical Information Service,
U. S. Department of Commerce, Springfield, Virginia
22161.

The findings in this report are not to be construed as
an official Department of the Army position, unless
so designated by other authorized documents.

*The use of trade names or manufacturers' names in this report
does not constitute endorsement of any commercial product.*

UNCLASSIFIED

SECURITY CLASSIFICATION OF THIS PAGE (When Data Entered)

REPORT DOCUMENTATION PAGE		READ INSTRUCTIONS BEFORE COMPLETING FORM
1. REPORT NUMBER	2. GOVT ACCESSION NO.	3. RECIPIENT'S CATALOG NUMBER
TECHNICAL REPORT ARBRL-TR-02527	ADA134740	
4. TITLE (and Subtitle)		5. TYPE OF REPORT & PERIOD COVERED
INTRACAVITY LASER EXCITATION OF NCO FLUORESCENCE IN AN ATMOSPHERIC PRESSURE FLAME		Final
		6. PERFORMING ORG. REPORT NUMBER
		8. CONTRACT OR GRANT NUMBER(s)
7. AUTHOR(s)		10. PROGRAM ELEMENT, PROJECT, TASK AREA & WORK UNIT NUMBERS
William R. Anderson, John A. Vanderhoff, Anthony J. Kotlar, Mark A. DeWilde, Richard A. Beyer		1L161102AH43
9. PERFORMING ORGANIZATION NAME AND ADDRESS		12. REPORT DATE
US Army Ballistic Research Laboratory ATTN: DRDAR-BLI Aberdeen Proving Ground, MD 21005		September 1983
11. CONTROLLING OFFICE NAME AND ADDRESS		13. NUMBER OF PAGES
US Army Armament Research & Development Command US Army Ballistic Research Laboratory (DRDAR-BLA-S) Aberdeen Proving Ground, MD 21005		43
14. MONITORING AGENCY NAME & ADDRESS (if different from Controlling Office)		15. SECURITY CLASS. (of this report)
		Unclassified
		15a. DECLASSIFICATION/DOWNGRADING SCHEDULE
16. DISTRIBUTION STATEMENT (of this Report)		
Approved for public release; distribution unlimited.		
17. DISTRIBUTION STATEMENT (of the abstract entered in Block 20, if different from Report)		
18. SUPPLEMENTARY NOTES		
19. KEY WORDS (Continue on reverse side if necessary and identify by block number)		
Laser Excited Fluorescence NCO Radical Combustion Diagnostics		
20. ABSTRACT (Continue on reverse side if necessary and identify by block number)		
1mn Laser excited fluorescence of the NCO radical has been obtained using discrete prism selected lines of an argon ion laser pump source. To our knowledge, this is the first time NCO fluorescence has been obtained in a flame environment. NCO was formed in a slightly rich atmospheric pressure CH ₄ /N ₂ O flame. This flame was placed inside the extended cavity of the argon laser to take advantage of the much higher light intensity levels. All of the available laser lines pump vibrational hot bands of the (CONT'D)		

DD FORM 1473

1 JAN 73

EDITION OF 1 NOV 65 IS OBSOLETE

UNCLASSIFIED

SECURITY CLASSIFICATION OF THIS PAGE (When Data Entered)

20. Abstract (Cont'd):

NCO A doublet-sigma-plus to X doublet-pi system. The 4658 Angstrom line appears to be the most useful for probing NCO densities. This line pumps from $v_1=1$ in the X state to the lowest vibrational level of the A state. NCO is pumped to N prime = 31 by this line, probably via the Q2(31) transition although the R2(30) and P2(32) transitions could not be ruled out in the present analysis. The 4658 Angstrom line was used to determine a relative NCO density profile through the reaction zone of a CH_4/N_2O flame. Profiles of C_2 , CN, and temperature were also obtained in this flame and are compared with the NCO profile. A lower limit of approximately $3 \times 10^{14} \text{ cm}^{-3}$ was placed on the peak NCO density in the flame. Attempts to find NCO or CN fluorescence in a CH_4 /air flame failed, indicating probable differences in nitrogen chemistry for the two flames.

TABLE OF CONTENTS

	<u>Page</u>
LIST OF FIGURES.....	5
I. INTRODUCTION.....	7
II. EXPERIMENTAL.....	9
III. RESULTS AND DISCUSSION.....	14
IV. CONCLUSIONS.....	31
ACKNOWLEDGEMENTS.....	33
REFERENCES.....	34
DISTRIBUTION LIST.....	37



Accession For	
NTIS	<input checked="" type="checkbox"/>
DTIC	<input type="checkbox"/>
Unannounced	<input type="checkbox"/>
Justification	<input type="checkbox"/>
By	
Distribution/	
Availability Codes	
Dist	Avail and/or Special
A-1	

LIST OF FIGURES

<u>Figure</u>	<u>Page</u>
1	Diagram of Burner Used for Laser Probing of Flames.....10
2	Cross Section Across Width of Burner.....11
3	Optical and Electronic Apparatus.....13
4	Flame Emission and LEF Spectra from a Slightly Rich CH ₄ /N ₂ O Flame Where the Resolution was 3 Å FWHM.....16
5	Flame Emission and LEF Spectrum of NCO Using the 4658 Å Laser Line.....17
6	High Resolution Fluorescence Scan (0.17 Å FWHM) of the Prominent Q ₂ Line Region.....19
7	High Resolution Fluorescence Scan (0.17 Å FWHM) of the Prominent Q ₁ and R ₁ Line Region.....21
8	High Resolution Fluorescence Spectrum of the NCO A ² Σ ⁺ (0, 0 ⁰ , 0) + X ² π (0, 0 ¹ , 0) Band Excited by the 4658 Å Laser Line.....22
9	LEF Spectrum in the Region of the 4658 Å Pump Line.....23
10	LEF Spectrum of NCO Using the 4765 Å Laser Line.....27
11	Measured Temperature and Relative Density Profiles of NCO, CN, and a ³ π _u C ₂ in a Slightly Rich CH ₄ /N ₂ O Flame.....30



I. INTRODUCTION

The NCO radical is thought to play an important intermediate role in hydrocarbon flames even though it has not been previously observed in a flame environment. In particular it is postulated that NCO is an intermediate in the conversion of fuel-bound nitrogen to NO_x and N_2 in rich combustion and in production of NO_x in hydrocarbon/air flames.¹ Our interest in NCO results from its possible importance in gun propellant flames. Experimental thermal decomposition studies of various gun propellants show that large quantities of HCHO, HCN, N_2O , and NO_2 are produced.² Thus flames³ composed of these fuels and oxidizers are of interest. Shock tube studies³ of the HCN + NO_2 system lead to the conclusion that an important pathway for the reaction involves NCO. For these reasons it is of interest to develop a sensitive technique for detection of NCO, in situ, in reactive systems.

NCO is the subject of several previous and contemporary spectral investigations. The A - X system was first identified in low resolution emission spectra upon photolysis of $\text{C}_2\text{H}_5\text{NCO}$ by Holland, et al.⁴ Subsequently, rotational analyses of the absorption spectra have been performed for the A - X system by Dixon⁵ and by Bolman et al.⁶ and for the $\text{B}^2\Pi - \text{X}^2\Pi$ system by

¹(a) G.B. Debrow, J.M. Goodings, and D.K. Bohme, "Flame-Ion Probe of Intermediates Leading to NO_x in $\text{CH}_4\text{-O}_2\text{-N}_2$ Flames," *Combustion and Flame*, Vol. 39, p. 1, 1980. (b) C. Morley, "The Mechanism of NO Formation from Nitrogen Compounds in Hydrogen Flames Studied by Laser Fluorescence," 18th Symposium (International) on Combustion, The Combustion Institute, Pittsburgh, PA, p.23, 1981. (c) Y.H. Song, D.W. Blair, V.J. Siminski, and W. Bartok, *ibid*, "Conversion of Fixed Nitrogen to N_2 in Rich Combustion," p. 53; and references therein.

²(a) R.A. Beyer, "Molecular Beam Sampling Mass Spectrometry of High Heating Rate Pyrolysis: Description of Data Acquisition System and Pyrolysis of HMX in a Polyurethane Binder," ARBRL-MR-02816, 1978 (AD A054328). (b) C.U. Morgan and R.A. Beyer, "ESR and IR Spectroscopic Studies of HMX and RDX Thermal Decomposition," 15th JANNAF Combustion Meeting, Newport, RI, September 1978.

³R.A. Fifer and H.E. Holmes, "Kinetics of the HCN + NO_2 Reaction Behind Shock Waves," to appear in *J. Phys. Chem.*

⁴R. Holland, D.W.G. Style, R.N. Dixon, and D.A. Ramsay, "Emission and Absorption Spectra of NCO and NCS," *Nature*, Vol. 182, p. 336, 1958.

⁵R.N. Dixon, "The Absorption Spectrum of the Free NCO Radical," *Phil. Trans. Roy. Soc.*, Vol. 252, p. 165, 1960.

⁶P.S.H. Bolman, J.M. Brown, A. Carrington, I. Kopp, and D.A. Ramsay, "A Re-Investigation of the $\text{A}^2\Sigma^+ - \text{X}^2\Pi$ Band System of NCO," *Proc. Roy. Soc.*, Vol. A343, p. 17, 1975.

Dixon.⁷ NCO A - X system emission, in addition to that from other species, has been used by Okabe⁸ to study photolysis of HNCO. In addition to these early gas phase experiments, NCO has been studied in matrix isolation experiments. Milligan and Jacox⁹ used this approach to investigate the infrared and ultraviolet absorption spectra. Bondybey and English¹⁰ similarly studied the laser excited fluorescence (LEF) spectra. More recently, in a paper mainly concerning a different subject, Reisler et al¹¹ reported gas phase radiative lifetimes of several vibrational levels of the A state. Finally, in a study not yet completed, Sullivan et al¹² have detected LEF for both the A and B states of NCO in a flow system. Preliminary measurements include A and B state lifetimes, collisional quenching rates for several added species, and ground vibrational state frequencies.

Recently, spontaneous Raman spectroscopy has been used to probe temperature and species profiles in premixed laminar CH₄/N₂O flames.¹³ During the course of these experiments intense laser fluorescences resulting from excitation with various prism selected lines of the probe argon ion laser were discovered. The radical species producing these fluorescences have been

⁷R.N. Dixon, "A² π - 2 π Electronic Band System of the Free NCO Radical," *Can. J. Phys.*, Vol. 38, p. 10, 1960.

⁸H. Okabe, "Photodissociation of HNCO in the Vacuum Ultraviolet; Production of NCO A³ π and NH (A³ π , c¹ π)," *J. Chem. Phys.*, Vol. 53, p. 3507, 1970.

⁹D.E. Milligan and M.E. Jacox, "Matrix Isolation Study of the Infrared and Ultraviolet Spectra of the Free Radical NCO," *J. Chem. Phys.*, Vol. 47, p. 5157, 1967.

¹⁰V.E. Bondybey and J.H. English, "Fermi Resonance and Vibrational Relaxation in the A² Σ State of NCO in Solid Argon," *J. Chem. Phys.*, Vol. 67, p. 2868, 1977.

¹¹H. Reisler, M. Mangir, and C. Wittig, "The Kinetics of Free Radicals Generated by IR Laser Photolysis. II. Reactions of C₂(X¹ Σ_g^+), C₂(a³ π_u), C₃(X¹ Σ_g^+) and CN(X² Σ^+) with O₂," *Chem. Phys.*, Vol. 47, p. 49, 1980.

¹²(a) B.J. Sullivan, G.P. Smith, D.R. Crosley, and G. Black, "Laser-Induced Fluorescence Studies of the NCO Molecule," *Eastern States Fall Technical Meeting of the Combustion Institute, Pittsburgh, PA, Paper 44, October 1981.*
(b) B.J. Sullivan, G.P. Smith, and D.R. Crosley, to be published.

¹³J.A. Vanderhoff, R.A. Beyer, and A.J. Kotlar, "Laser Raman Spectroscopy of Flames; Temperature and Concentrations in CH₄/N₂O Flames," ARBRL-TR-02388, January 1982 (AD A112326).

identified as C_2 , CN and NCO.¹⁴⁻¹⁷ Measurements involving C_2 and CN¹⁵ concentrations and CN $B^2\Sigma^+$ energy transfer¹⁶ in the flame are discussed in separate papers. This paper addresses the spectral identification and concentration profile of NCO in the flame. The present work includes a more detailed description of the apparatus and discussion of the results than appeared previously.¹⁷ Two major issues are addressed. First, the best argon laser line for probing NCO densities and the transition it pumps are discussed. Then, an accurate relative density profile is presented along with an estimate of the absolute peak NCO density for our flame conditions. The estimate, which is thought to be good to about a factor of 5, places a lower bound on the NCO density of $\sim 3 \times 10^{14} \text{ cm}^{-3}$ in our slightly rich flame.* This density is sufficiently large that possible participation of NCO in the flame chemistry should be considered.

II. EXPERIMENTAL

A. Burner

Rich premixed flames of methane and nitrous oxide burning at atmospheric pressure have been studied using an open channel curved knife edge burner shown in Figures 1 and 2. The burner was recently designed in this laboratory for intracavity laser probing through the reaction zone of premixed flames.¹⁸ The burner was made from two aluminum plates with various gaskets providing the desired channel width. For these experiments the rectangular channel dimensions were 50 mm by 3 mm. Two small, independent channels run along each side of the main channel and a flow of N_2 through these channels prevents the flame from wrapping around the ends of the knife edges. The burner produces a curved flame front which follows the radius of curvature of the knife edges (50.8 mm). In typical usage a laser beam passes between the knife edges parallel to the top of the burner (Figure 1b). The cross section

¹⁴J.A. Vanderhoff, R.A. Beyer, W.R. Anderson, and A.J. Kotlar, "Ar⁺ Laser Excited Fluorescence Profiles of Radicals Produced in a CH_4/N_2O Flame," 36th Symposium on Molecular Spectroscopy, Columbus, Ohio, June 1981.

¹⁵J.A. Vanderhoff, R.A. Beyer, A.J. Kotlar, and W.R. Anderson, "Ar⁺ Laser Excited Fluorescence of C_2 and CN Produced in a Flame," to appear in *Combustion and Flame*.

¹⁶W.R. Anderson, A.J. Kotlar, and J.A. Vanderhoff, to be published.

¹⁷W.R. Anderson, J.A. Vanderhoff, A.J. Kotlar, L.J. Decker, and R.A. Beyer, "Laser Excitation of NCO A - X System Fluorescence in a CH_4/N_2O Flame Using an Argon Ion Laser," Eastern States Fall Technical Meeting of the Combustion Institute, Pittsburgh, PA, Paper 47, October 1981.

*Compare this to the overall flame molecular density of $\sim 3 \times 10^{18} \text{ cm}^{-3}$ at 1 atm and the measured flame temperature, 2500 K.

¹⁸R.A. Beyer and M.A. DeWilde, "Simple Burner for Laser Probing of Flames," *Rev. Sci. Instrum.*, Vol. 53, p. 103, 1982.

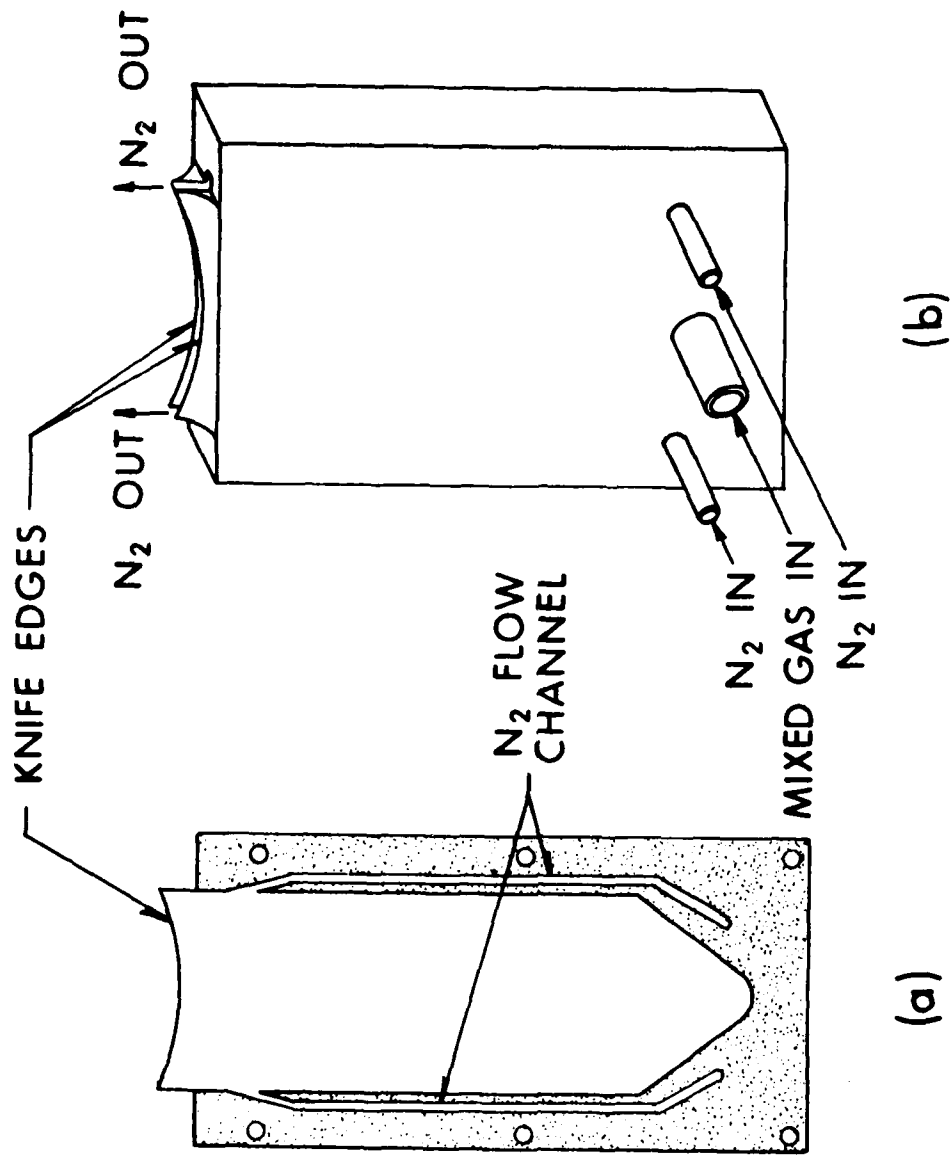


Figure 1. Diagram of Burner Used for Laser Probing of Flames. a. Lengthwise cross section of burner showing large central channel for premixed gases and small N₂ flow channels. b. Outside view of burner.

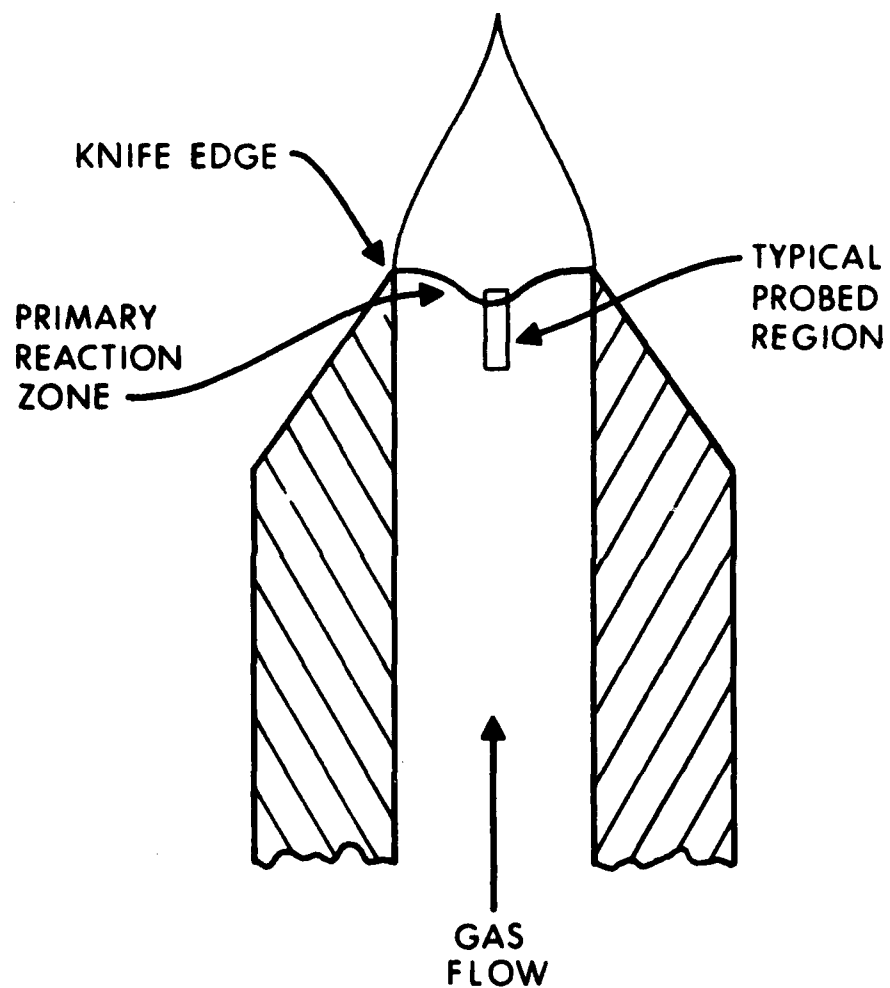


Figure 2. Cross Section Across Width of Burner. A typical flame position is shown. The laser beam is circular in cross section. The rectangular area labeled "typical probed region" was mapped out by moving the burner back and forth through the laser beam.

in Figure 2 shows a typical laser beam position. For the present experiments, only a length of about 3 mm of the laser beam was viewed by the detection optics. Since the radius of curvature of the knife edges is much larger than this, the results may be treated using one-dimensional flame approximations. The curvature is used to minimize index of refraction effects on the laser beam.

Gas flow to the burner is regulated by rotameters. The fuel oxidizer mixture is expressed as an equivalence ratio ϕ , where ϕ is defined as the actual fuel-oxidizer concentration ratio divided by the stoichiometric fuel-oxidizer concentration ratio (i.e., $4 [\text{CH}_4]/[\text{N}_2\text{O}]$). The spectroscopic results for NCO were obtained at different times without an emphasis being placed on the exact flame conditions. Here the approximate conditions were $\phi = 1.6$ with 40% dilution by mole fraction with N_2 . For the case where the concentration and temperature profiles and the absolute density estimates were obtained the flow conditions were carefully measured with a wet test meter. The results were $\phi = 1.36 \pm 0.02$ with 45% dilution with N_2 . The overall premixed gas flow rate was 1.72 ± 0.05 l/min at 298 K and 1 atmosphere.

Temperature measurements performed on this burner using spontaneous Raman spectroscopy indicate that heat losses to the burner are very small.¹⁸ That is, within experimental error ($< 50\text{K}$) the maximum flame temperatures measured are the same as obtained from an equilibrium flame temperature calculation assuming adiabatic conditions.

B. Optics and Electronics

The experimental arrangement for this study is shown in Figure 3. A nominal 4 watt (all lines) argon ion laser with prism line selection was used as the excitation source. Its cavity was extended with two highly reflective mirrors of focal length 1 m and 0.3 m providing an intracavity beam waist of about 100 μm . The intracavity circulating power was about 50 watts on the strongest lines. Only minor attenuation occurred when a steady $\text{CH}_4/\text{N}_2\text{O}$ flame was inserted in the cavity at the beam waist. The burner was placed on its side with the open channel facing the detection optics. The burner was attached to a small milling table providing movement in two directions. For the flame profiles measured in the present work the burner motion was along the line of sight of the detection optics. This motion was monitored using a precision dial gauge which reads directly to 0.01 mm.

For coarse spectral resolution (see Fig. 3) two quartz lenses were used to image a portion of the scattered light onto the 100 μm horizontal slits of a 0.25 m spectrometer mounted on its side. The sampled light came from a volume approximated by a cylinder of 100 μm diameter and 3 mm in length. An optical multichannel analyzer (OMA) with a silicon intensified vidicon tube was used to detect the dispersed light. Using a grating of 1180 grooves/mm approximately 400 \AA of the spectrum could be observed at one time with this system. The radiation was accumulated into 500 channels which, when coupled with the 100 μm entrance slits of the spectrometer, provided a resolution, FWHM, of approximately 3 \AA . The data was accumulated for equal lengths of time into the two separate OMA memories first with laser on and then with laser off conditions. The latter provided a flame background emission spectrum. Differencing of these two memories yielded the LEF or Raman spectrum. Accumulation times for data reported here were usually less than

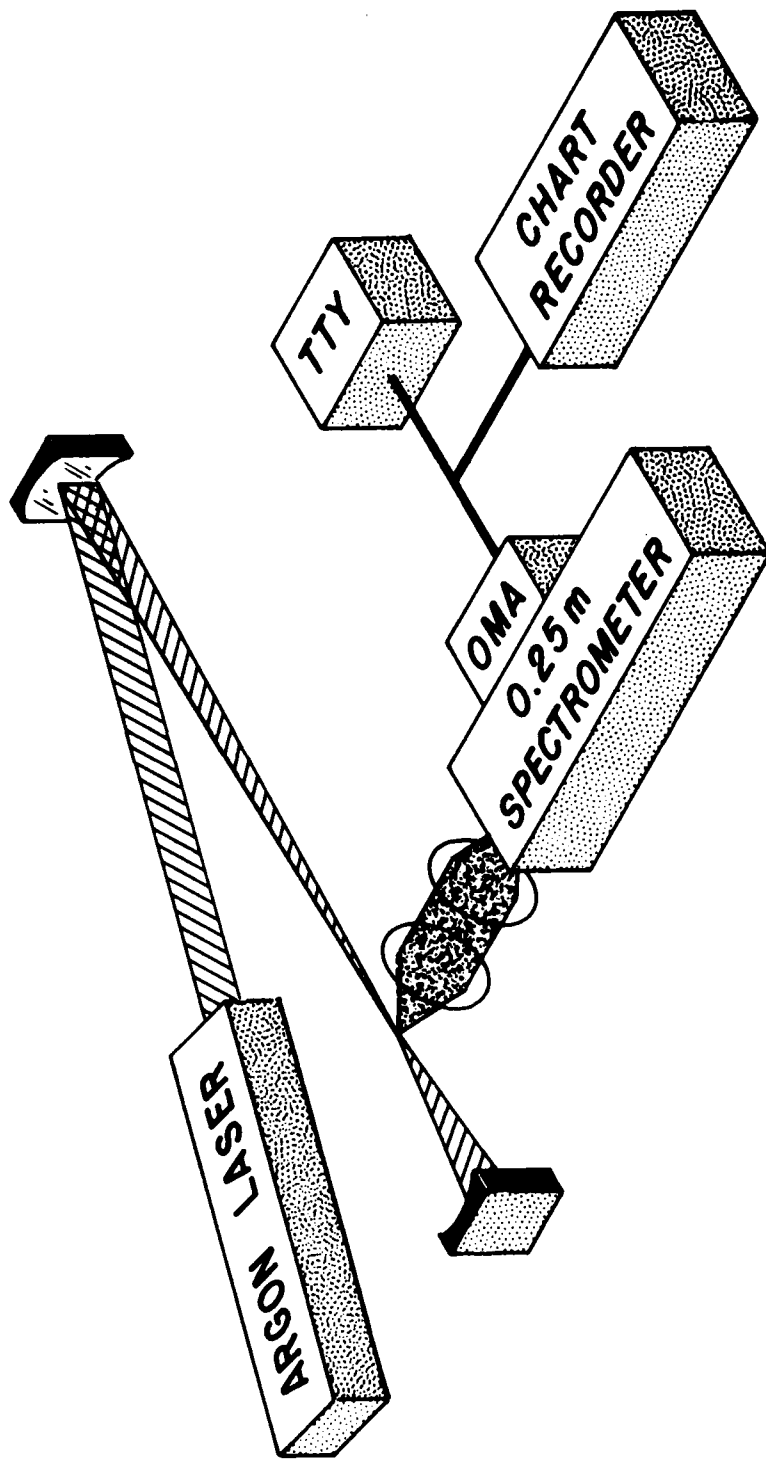


Figure 3. Optical and Electronic Apparatus. Two concave mirrors were used to extend the cavity of an argon ion laser. A flame (not shown) was placed at the intracavity focal point. Scattered radiation was focussed onto the slits of a 0.25 m monochromator with OMA detector. Output from the OMA was viewed on a recorder. Hard copy was obtained on a teletype.

ten seconds for LEF and about thirty seconds for Raman scattering data. Frequently, neutral density filters had to be placed in front of the entrance slits of the monochromator to keep the real time LEF signal within the dynamic range of the OMA. Either LEF or Raman signals from the reaction zone of the flame could be readily observed in real time on a display oscilloscope. Our discovery of these unexpected fluorescences may be directly traced to this capability.

While the 0.25 m spectrometer - OMA detection system had sufficient resolution to allow identification of C_2 and CN,^{14,15} the rotational structure of NCO was much too dense to allow a firm assignment of the spectrum. For this reason a higher resolution detection system was necessary. Here a 1 m monochromator with a cooled EMI type 9789 QA photomultiplier tube (PMT) wired for photon counting replaced the 0.25 m monochromator - OMA system in Figure 3. A chopper operating at 40 Hz was placed inside the laser cavity to provide laser on and laser off conditions necessary for the elimination of the background signal. A glass dove prism was placed in front of the entrance slits to rotate the image 90°. The highest resolution achieved with this system was 0.17 Å FWHM. Amplified pulses from the photomultiplier tube were passed through a single channel analyzer which discriminated against noise sources. The output of the single channel analyzer then passed through, in parallel, two linear gates and two rate meters. The flame background was removed from the LEF signal by gating the signal to the two rate meters in synch with the chopper and subtracting the rate meter outputs. The response time of the ratemeters was such that these signals appeared continuous and could thus be subtracted easily. The resultant LEF (difference) and flame emission signals were recorded with a dual strip chart recorder. In addition, the separate ratemeter outputs could be digitized and stored in a PDP 11/34 computer for later analysis.

III. RESULTS AND DISCUSSION

A. Interpretation of Spectral Features

As mentioned in the introduction the LEF spectra of NCO were first observed while measuring temperature and major species profiles in a flame using spontaneous Raman spectroscopy. Some typical OMA spectra from this early work¹⁴ are shown in Figure 4. The upper trace is a flame emission spectrum obtained with the laser blocked. Most of the emission observed is from the $\Delta v = -1$ sequence of the CN $B^2\Sigma^+ + X^2\Sigma^+$ violet system (4140 - 4220 Å) or from the $\Delta v = 0$ sequence of the CH $A^2\Delta + X^2\Pi$ system (4240-4400 Å). Higher resolution scans, shown later, indicate that a small fraction of the emission in the CH P-branch region is due to NCO. Fluorescence spectra obtained by subtracting this emission spectrum from the fluorescence plus emission spectra are shown for seven discrete Ar⁺ laser pump lines. These individual spectra were normalized and are thus not of similar intensity as depicted in Figure 4.

Inspection of the fluorescence spectra of Figure 4 reveals several interesting features. First, one of the laser lines, 4545 Å, pumps CN. Fluorescence from the R and P branches of the (1,2) band in the B - X system results in the two sharp peaks between 4160 and 4200 Å. Studies described in detail elsewhere¹⁵ showed that the 4545 Å line pumps a (1,3) R 20 transition of CN. Second, apart from the CN band, all of the fluorescence spectra

consist of a system of bands in an envelope extending from about 4160 - 4440 Å. Similar appearing band envelopes are also obtained when pumping with the 4965 and 5145 Å lines (not shown). These spectra look similar to the NCO emission spectra observed by Okabe⁸ upon photolyzing HNCO. It was for this reason that we originally, tentatively, assigned the spectra to NCO.¹⁴

The fluorescence spectrum from the 4658 Å pump line was initially selected for detailed examination using the 1 m monochromator for two reasons. First, the shape of the envelope for the banded system is quite different and appears narrower than that from the other pump lines. (See Figure 4.) Second, the integrated fluorescence intensity (unnormalized for laser power) is the strongest for the 4658 Å pump line in spite of the fact that this is one of the weakest laser lines. This intense fluorescence may be understood by examining earlier fluorescence and absorption work on NCO. Bondybey and English¹⁰ observed fluorescence of matrix isolated NCO by pumping to the $A^2\Sigma^+(0,0^0,0)$ state. The resulting fluorescence to the $X^2\Pi(1,0^1,0)$ state occurs between 21,300 - 21,600 cm^{-1} , a range encompassing the 4658 Å laser excitation line. Additional confirmation that the 4658 Å laser line pumps to the $A^2\Sigma^+(0,0^0,0)$ vibrational state comes from experimental absorption results combined with determinations of the $X^2\Pi(1,0^1,0)$ energy. Absorption studies^{5,6} of gas phase NCO show that the $A^2\Sigma^+(0,0^0,0) + X^2\Pi(0,0^1,0)$ transition lies in the frequency region 22,700 - 22,900 cm^{-1} . Combining this result with the average of three measurements of the $X^2\Pi(1,0^1,0)$ energy level,^{9,10,12} 1274 cm^{-1} , indicates that the 4658 Å line falls in the right region for $A^2\Sigma^+(0,0^0,0) + X^2\Pi(1,0^1,0)$ excitation of NCO. None of the other laser lines overlap such a low-lying vibrational band so well, explaining the stronger fluorescence observed upon pumping with the 4658 Å line.

A scan of the fluorescence from the 4658 Å pump line using the 1 m monochromator at 0.60 Å FWHM resolution is shown in Figure 5. The top trace is flame emission resulting primarily from the CH A - X (0,0) P-branch. The lower trace is the LEF spectrum. The spectra are of similar intensity, as shown, demonstrating the necessity for subtracting the flame emission. Seven bandheads from two vibrational bands previously observed in absorption experiments on the NCO A + X system^{5,6} may be readily identified in the fluorescence spectrum. Thus the previous tentative assignment to NCO is confirmed. In addition, 8 prominent lines are observed at regularly spaced intervals of about 4.5 Å in the spectrum. Two of these lines are only resolved from the bandheads in scans at the highest resolution available (0.17 Å FWHM). They are slightly to the violet of the P_1 and P_2 bandheads in Fig. 5. This pattern of lines is an indication that the number density in a rotational state of $A^2\Sigma^+(0,0^0,0)$ having quantum number $N' = 30$ or 31 is much larger than for any other rotational state. It is common in a flame environment for a rotational level directly pumped by an excitation source in an electronically excited molecule to retain a higher population than nearby

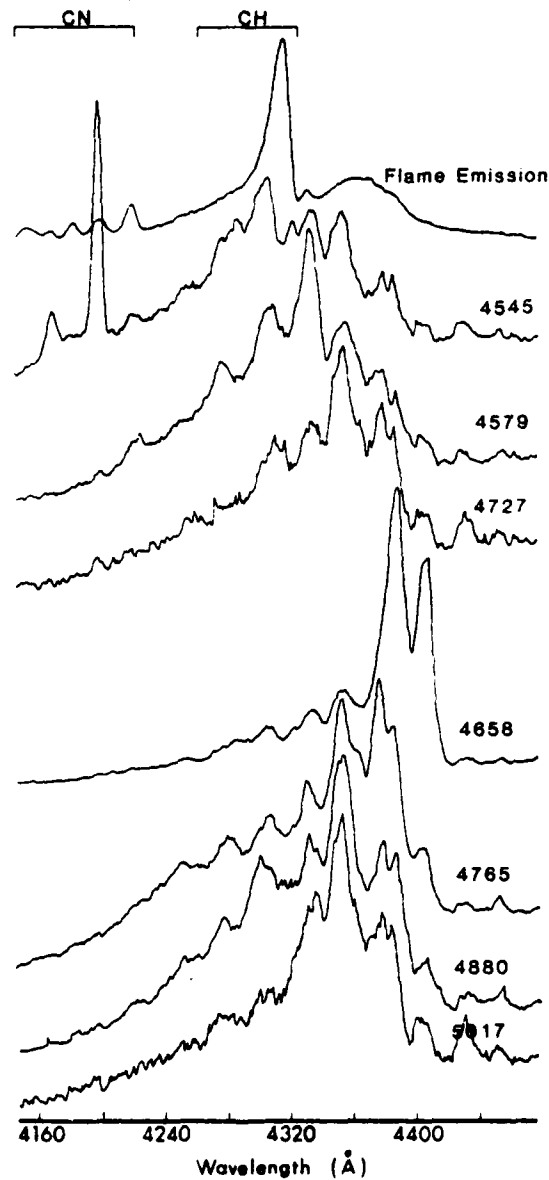
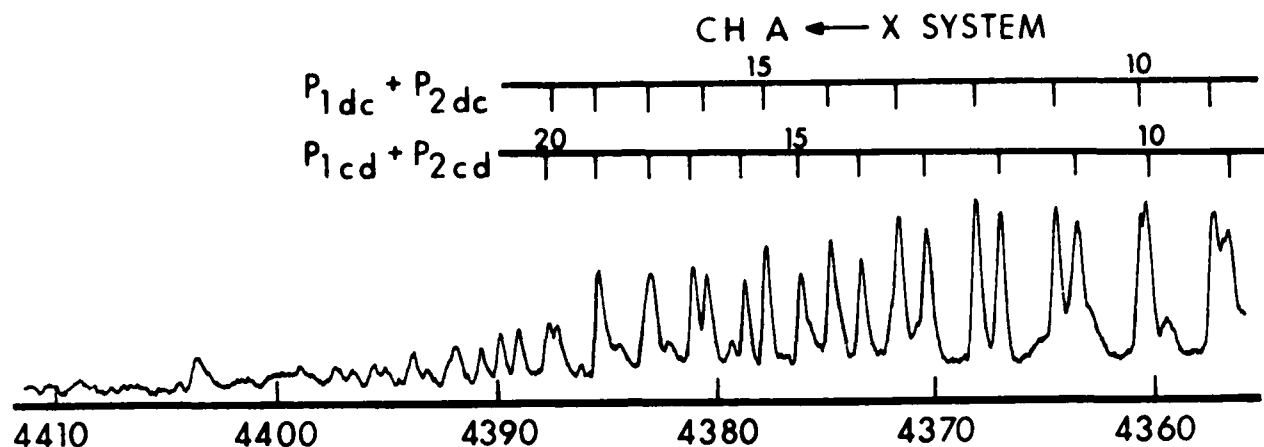


Figure 4. Flame Emission and LEF Spectra from a Slightly Rich $\text{CH}_4/\text{N}_2\text{O}$ Flame Where the Resolution was 3\AA FWHM. The spectra have been normalized so that no information about relative intensities of LEF from the various argon pump lines may be obtained from the figure. The top trace is the flame emission. The other seven traces are LEF spectra resulting from the argon laser pump lines indicated to the right.

EMISSION



NCO FLUORESCENCE 4658 Å PUMP

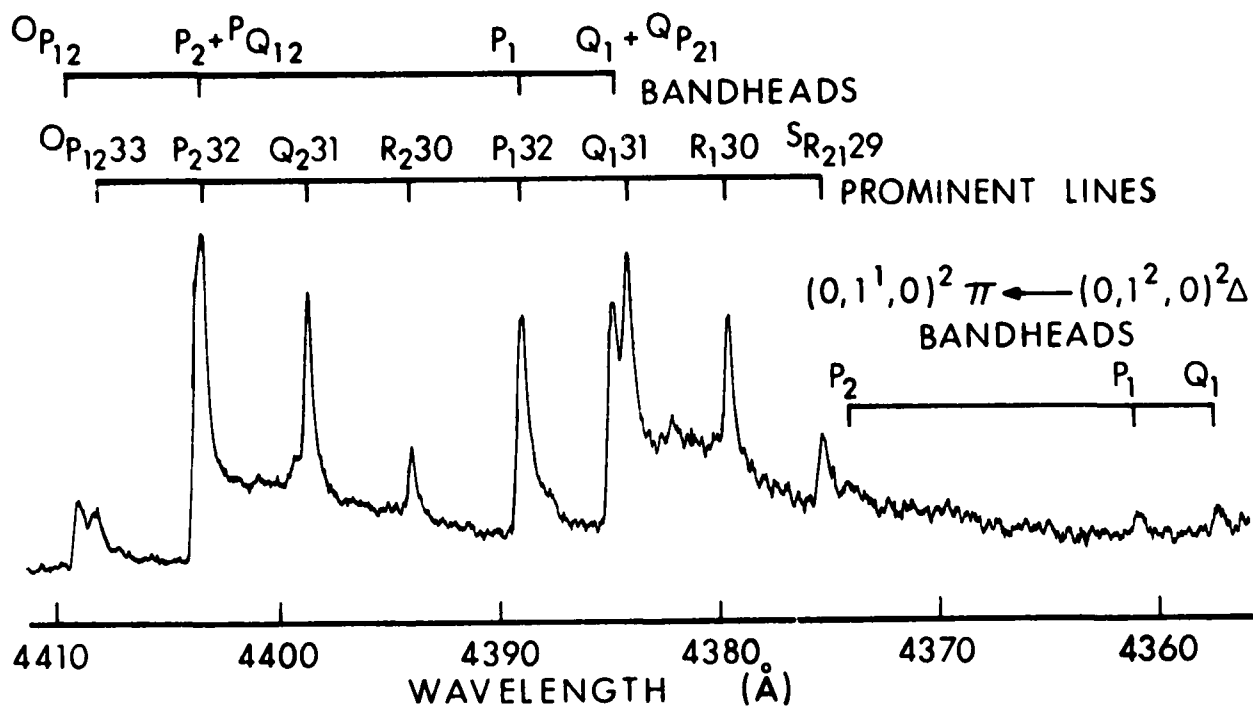
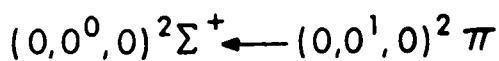


Figure 5. Flame Emission and LEF Spectrum of NCO Using the 4658 Å Laser Line. The spectra were taken at a resolution of 0.60 Å FWHM. Top trace: Flame emission arising mainly from the CH A ← X system. Some weaker bandheads of NCO are also visible. Bottom trace: LEF spectrum of NCO in the $\Delta v = 0$ region.

levels. This is demonstrated by fluorescence scans on OH,^{19,20} CH,²¹ CN^{16,21} and by indirect evidence from an excitation scan on NH for which the detector was biased towards fluorescence from only a few rotational levels.²² This phenomenon demonstrates that rotational energy transfer in the excited state is not sufficiently fast to redistribute molecules to a Boltzmann distribution before they are quenched to the ground state.^{16,19,20}

Evidence that $N' = 31$ is the level pumped by the 4658 Å excitation line is given in Figures 6 and 7. Under serendipitous conditions argon discharge lines²³ at 4401.02 Å and 4400.09 Å appeared in the spectrum. A section from one spectrum at 0.17 Å FWHM resolution in which these lines appeared is shown in Figure 6. These Ar⁺ lines are very close to the prominent Q₂ line and were used to calibrate* the prominent line position as 4398.41 Å. The position measured by Dixon⁵ for Q₂31 was 4398.36 Å. (Measured line positions and assignments of Reference 5 and 6 for this band are in excellent agreement.) Separation between adjacent Q₂ lines in this region is about 0.21 Å, so that the precision of the calibration is sufficient to rule out other assignments. Thus, the prominent Q₂ line is established as Q₂31.

¹⁹C. Chan and J.W. Daily, "Laser Excitation Dynamics of OH in Flames," Applied Opt., Vol. 19, p. 1357, 1980.

²⁰G.P. Smith and D.R. Crosley, "Quantitative Laser-Induced Fluorescence in OH: Transition Probabilities and the Influence of Energy Transfer," 18th Symposium (International) on Combustion, The Combustion Institute, Pittsburgh, PA, p. 1511, 1981.

²¹A.C. Eckbreth, P.A. Bonczyk, and J.F. Verdieck, "Investigation of CARS and Laser-Induced Fluorescence for Practical Combustion Diagnosis," Report No. EPA - 600/7-80-091, May 1980. Example spectra abstracted from this report may be found in: A.C. Eckbreth, "Spatially Precise Laser Diagnostics for Practical Combustor Probing," Laser Probes for Combustion Chemistry, edited by D.R. Crosley, American Chemical Society Symposium Series 134, Washington, D.C., p. 271, 1980; J.F. Verdieck and P.A. Bonczyk, "Laser-Induced Saturated Fluorescence Investigations of CH, CN and NO in Flames," 18th Symposium (International) on Combustion, The Combustion Institute, Pittsburgh, PA, p. 1559, 1981.

²²W.R. Anderson, L.J. Decker, and A.J. Kotlar, "Concentration Profiles of NH and OH in a Stoichiometric CH₄/N₂O Flame by Laser Excited Fluorescence and Absorption," to appear in Combustion and Flame.

²³Atomic line positions were obtained from G.R. Harrison, Massachusetts Institute of Technology Wavelength Tables, M.I.T. Press, Cambridge, MA, 1969.

*It was discovered that the monochromator scan was not quite linear over long wavelength regions. The spectra in Figures 5, 7, and 8 were scanned from longer to shorter wavelengths. Towards the shorter wavelengths, the scans are only good to within about ±0.5Å. Therefore, high resolution scans were calibrated using known line positions of argon and CH emission. The calibration lines were chosen so that only short wavelength scans were required.

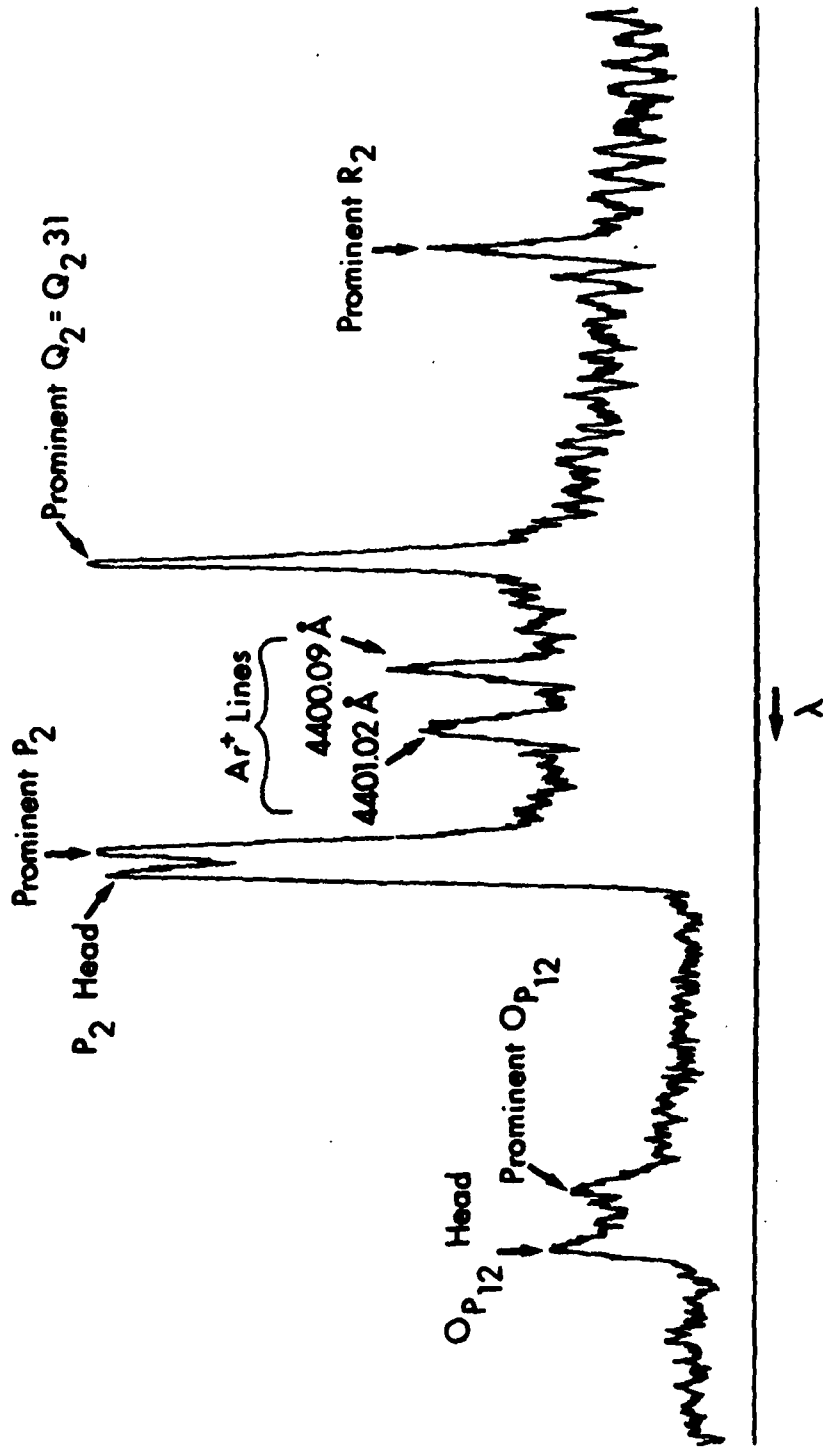


Figure 6. High Resolution Fluorescence Scan (0.17 Å FWHM) of the Prominent Q₂ Line Region. The two Ar⁺ discharge lines were used to calibrate the prominent Q₂ line position.

As a crosscheck on the identification of the prominent Q_2 branch line a scan at 0.17 Å FWHM resolution was made in the region of the prominent Q_1 and R_1 line positions. These positions were checked against nearby known CH line positions (see Figures 5 and 7) obtained from the work of Moore and Broida.²⁴ If the assignment of $N' = 31$ as the pumped level is correct, the prominent Q_1 and R_1 branch lines would be Q_131 and R_130 . The CH P_{cd18} and $P_{dc18} + P_{cd19}$ were used to calibrate the position of the Q_1 line as 4383.89 Å, while the CH P_{cd16} and P_{dc16} were used to calibrate the position of the R_1 line* as 4379.21 Å. The positions measured by Dixon⁵ for Q_131 and R_130 were 4383.91 and 4379.22 Å, respectively. Separations between adjacent Q_1 and R_1 lines near $N' = 31$ are about 0.10 and 0.40 Å, respectively. Thus, the Q_1 line position is most consistent with an assignment of Q_131 . However, the calibration is not precise enough to rule out Q_130 or Q_132 as the lines are so dense near the bandhead. This is not the case for the R_1 line as it is not near a bandhead. The separations between R_1 lines are large enough to allow firm identification of the prominent line as R_130 . Therefore, all of the prominent lines of Figure 5 must arise from $N' = 31$. Those lines not identified by direct calibration were labeled on the basis that $N' = 31$ is the level pumped by the laser. A full high resolution scan (0.17 Å FWHM) of the $A^2\Sigma^+(0,0^0,0) + X^2\Pi(0,0^1,0)$ fluorescence using the 4658 Å laser pump line is shown in Figure 8. The series of small, regularly spaced peaks about the prominent Q_2 line is due to the Q_2 branch progression.** The similar Q_1 branch progression is not well resolved because the Q_1 lines are more closely spaced.^{5,6}

Efforts were made to identify the rotational branch pumped by the 4658 Å laser line and, hence, the (N'' , J'') level from which pumping occurs. For this purpose, spectra were taken at 0.60 Å resolution in the region of the laser excitation line. An example is shown in Figure 9. The strong peak at 4658 Å is due to scattered laser light. The peak drops to zero at line center because of saturation of the detection electronics. Three pairs of peaks positioned symmetrically about the pump line are grating ghosts and should be disregarded. The remainder of the spectrum is complicated by LEF from the C_2 Swan system.¹⁵ Here the 4658 Å line excites in the (2,1) band. Because the C_2 emission is much stronger than the NCO emission in this region we were able to compare the emission and fluorescence spectra ascribing peaks which occur in both to C_2 . Grating ghosts were also eliminated from consideration. The remaining peaks (except for the laser line) are designated with arrows in Figure 9.

²⁴C.E. Moore and H.P. Broida, "CH in the Solar Spectrum," J. Res. Nat. Bur. Stand., Vol. 63A, p. 19, 1959.

*In the text, F-number subscripts for CH transitions are dropped for convenience since spin-orbit components were overlapped even at our highest available resolution.

**At first glance the reproducibly larger size of the Q_232 compared to Q_230 in Figure 8 suggests preferential rotational up-transfer, which seems unreasonable. The large size of Q_232 is probably due to overlap with the R_216 . The laser line width is much too narrow to pump $N' = 31$ and 32 simultaneously.

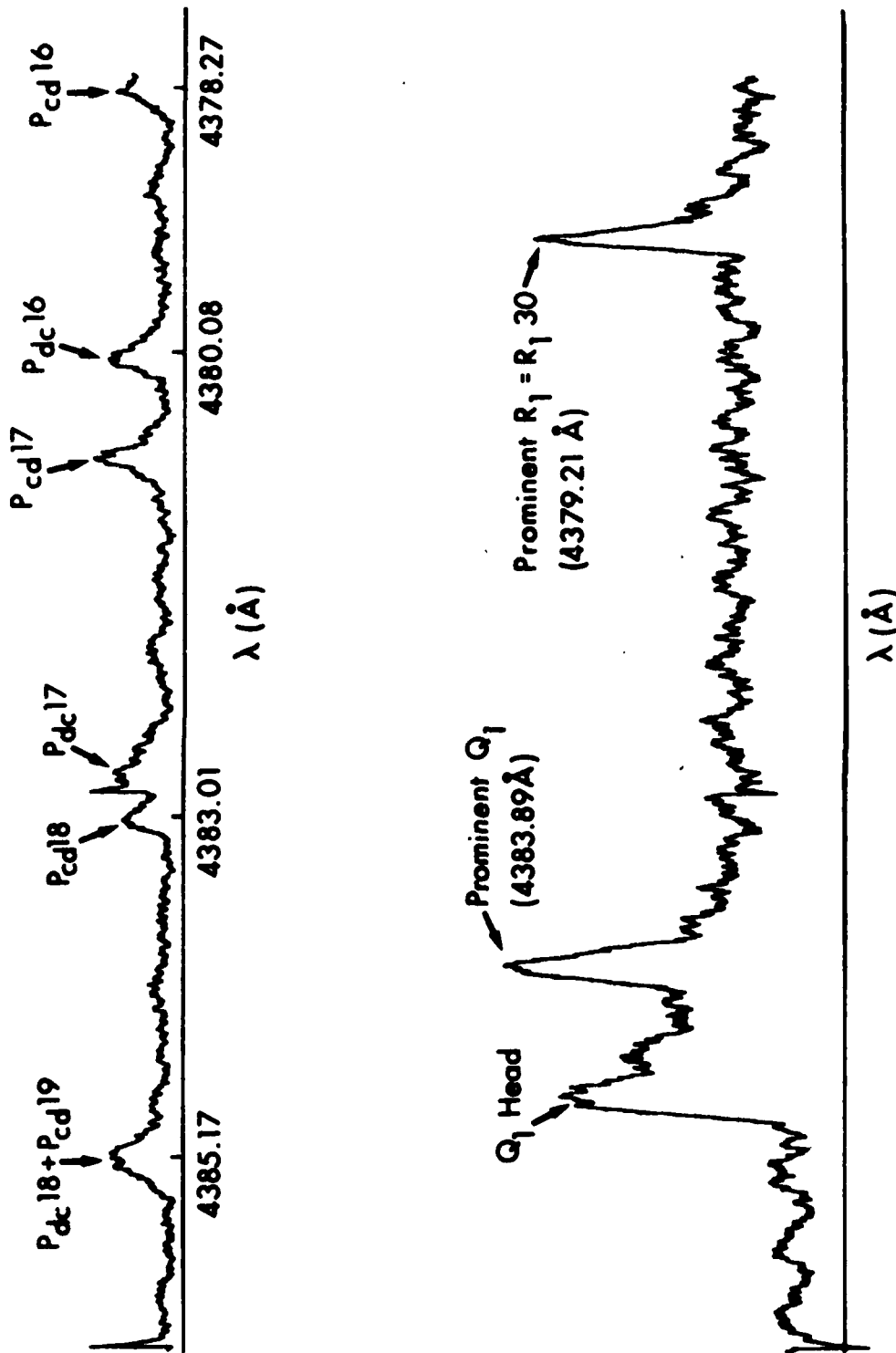


Figure 7. High Resolution Fluorescence Scan (0.17 \AA FWHM) of the Prominent Q_1 and R_1 Line Region. Top trace: CH flame emission. Bottom trace: NCO fluorescence spectrum. Results of calibrations of the prominent Q_1 and R_1 line positions using known CH wavelength²⁴ are shown.

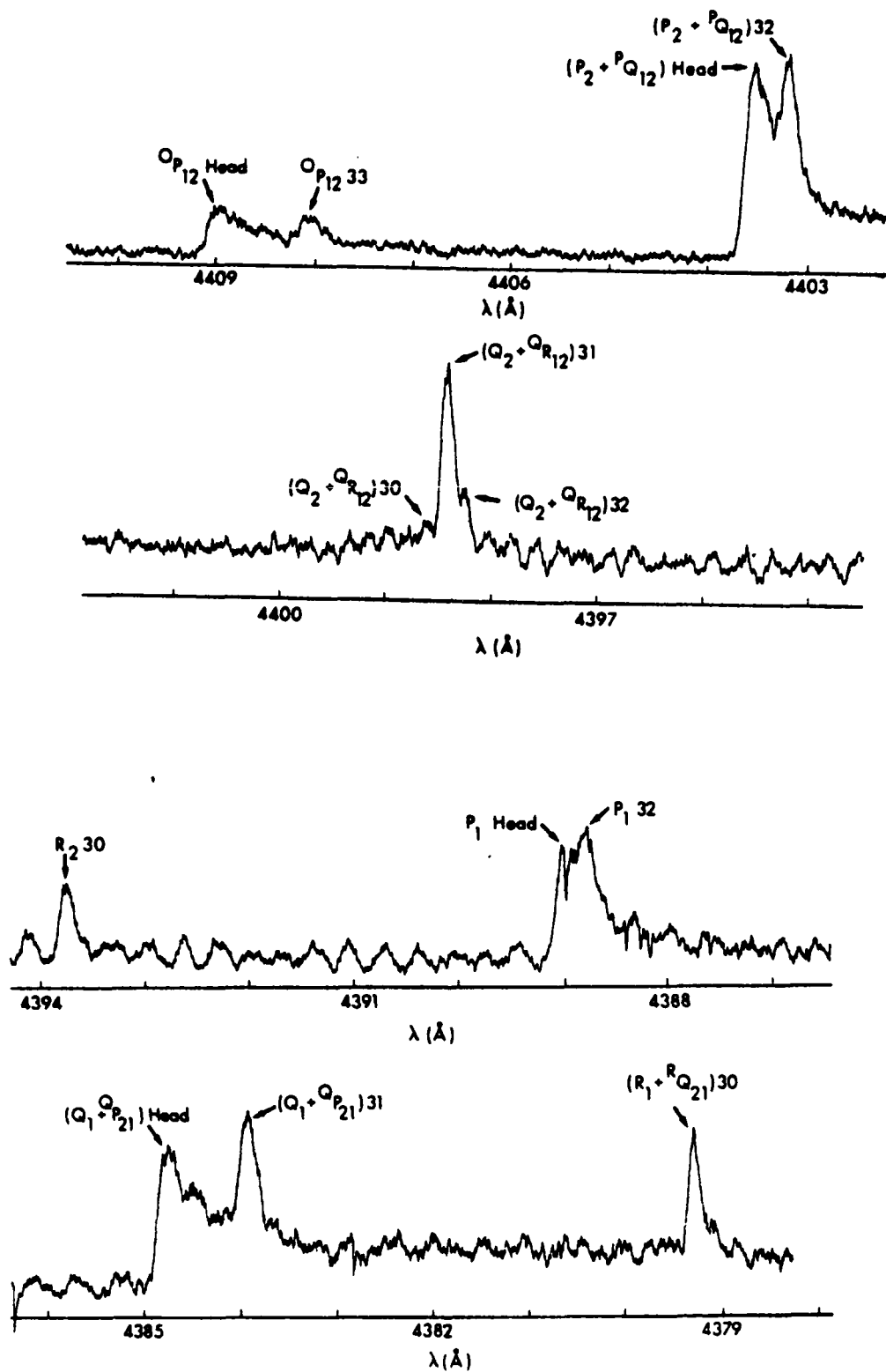


Figure 8. High Resolution Fluorescence Spectrum of the $\text{NCO } A^2\Sigma^+(0, 0^0, 0) \leftarrow X^2\Pi(0, 0^1, 0)$ band Excited by the 4658 \AA Laser Line. Wavelengths are only approximate due to irregularity in the monochromator scanning mechanism. (See footnotes to text.)

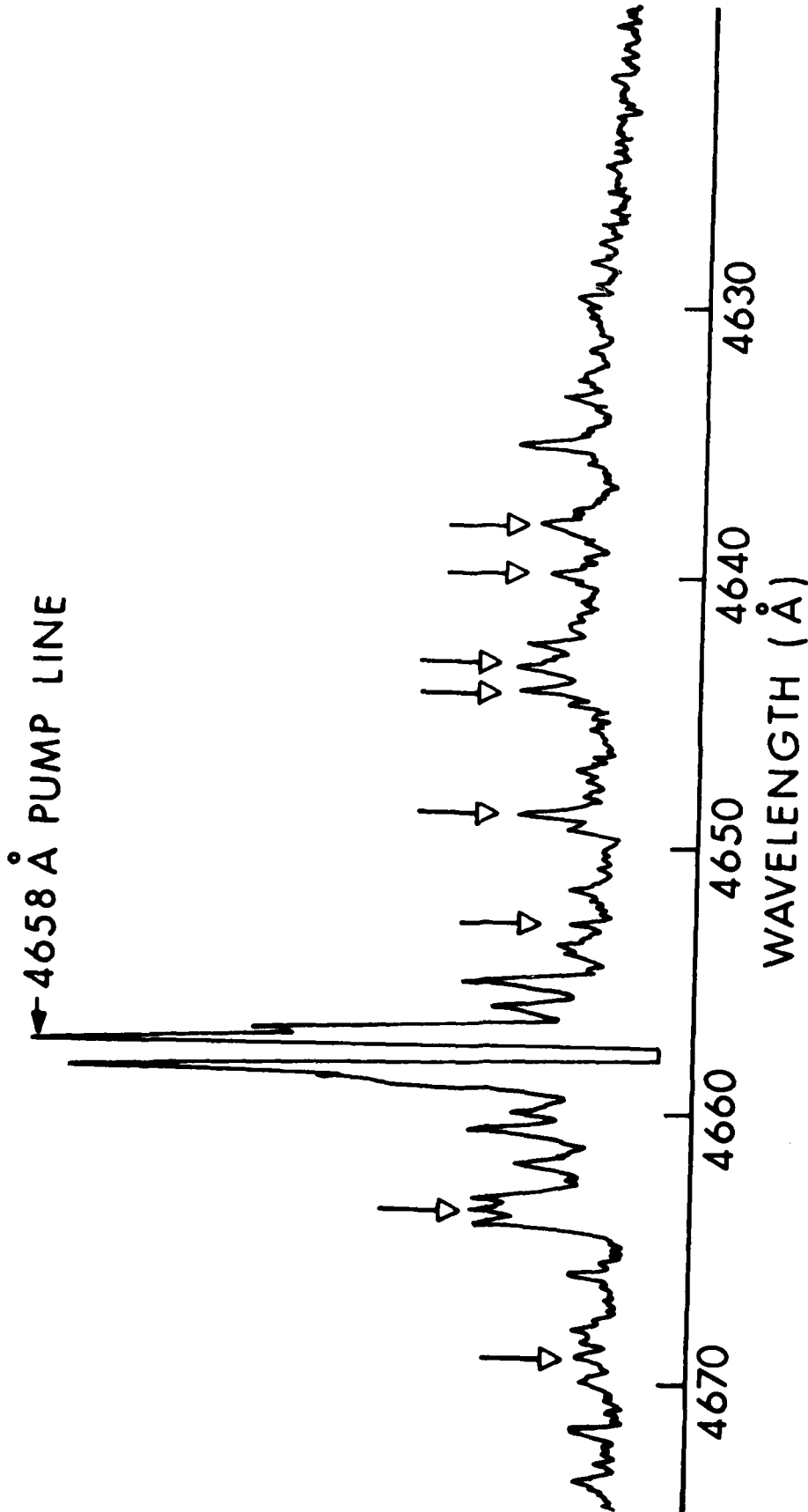


Figure 9. LEF Spectrum in the Region of the 4658 Å Pump Line. The spectrum was taken at 0.60 Å FWHM resolution. The scattered light from the Laser line dropped to zero due to saturation of the detection electronics. Three pairs of peaks placed symmetrically about the pump line were attributed to grating ghosts. Of the remaining peaks, those labeled with arrows are not present in the flame emission spectrum which, in this region, is mainly due to C₂.

The following observations may help interpret the spectrum of Figure 9. Emission in the 4400 Å region results from the $A^2\Sigma^+(0,0^0,0) + X^2\Pi(0,0^1,0)$ vibrational band. The $A^2\Sigma^+(0,0^0,0) + X^2\Pi(1,0^1,0)$ band has the same overall symmetries of ground and excited states. Though no rotational analysis for the $X^2\Pi(1,0^1,0)$ state is available, one would expect its rotational constants to be nearly the same as those for the $X^2\Pi(0,0^1,0)$ state. Therefore, the rotational branch structure of these two vibrational bands should be quite similar. In particular, though minor differences might well occur, the relative spacings and intensities of the bandheads and prominent lines from $N' = 31$ should be about the same for the two vibrational bands. Thus if spectra for both bands are available on the same wavelength scale, an overlay of the two spectra should reveal similarities. (Note, of course, that the pumped transition will lie directly under the laser line.) We have overlaid transparencies of the spectra and compared them as described. This comparison leads to the best agreement when one assumes the Q_2 branch line is pumped. However, the assignment is not firm due to the C_2 and grating ghost interferences in Figure 9.

Because of the expected similarities in rotational structure for the two vibrational bands of interest in the preceding paragraph, one can compute approximate positions of rotational lines in the $A^2\Sigma^+(0,0^0,0) + X^2\Pi(1,0^1,0)$ band by subtracting the energy of $X^2\Pi(1,0^1,0)$, 1274 cm^{-1} , from the energy for the corresponding rotational line in the $A^2\Sigma^+(0,0^0,0) + X^2\Pi(0,0^1,0)$ band. This has been done for all possible lines having $N'=31$. The result is shown in Table 1. The $A^2\Sigma^+(0,0^0,0) + X^2\Pi(0,0^1,0)$ line positions were obtained from the absorption spectra.^{5,6} The 4657.94 Å laser line²³ corresponds to an energy of 21463 cm^{-1} . This clearly matches the estimated Q_{231} position best, in agreement with the overlay result. The slight discrepancy is not unreasonable considering the assumption of equal rotational constants for the two vibrational levels. However, the assignment of transition type as Q_2 is still not entirely conclusive. The error limits on measurements of the $X^2\Pi(1,0^1,0)$ energy are large enough that assignment of the pumping transition to the P_{232} or R_{230} cannot be ruled out. Though assignment to other than the Q_2 branch seems unlikely, a firm identification awaits further study.

The prominent lines in the spectrum in Figure 5 also yield information about energy transfer in the excited NCO. As shown, the Q_{131} and Q_{231} intensities are nearly equal. Since one would expect nearly equal rotational line strengths for these transitions, these intensities indicate approximately equal densities in the F_1 and F_2 spin components for $N' = 31$, in contrast to observations made for the $A^2\Sigma^+$ state of OH in a flame.²⁰ These equal populations may arise either by excitation to one spin state followed by rapid spin state redistribution with retention of N' identity, or by equal pumping of two spin states via overlap of main and satellite branch transitions. A calculation of the excited state spin-splitting using the spin-rotation constant of Ref. 6 yields $F_{131} - F_{231} = 0.016 \pm 0.005 \text{ cm}^{-1}$. Since the Doppler width at the measured flame temperature of 2500 K is about 0.13 cm^{-1} , the main branch and satellite transitions are almost completely overlapped under these conditions. If pumping occurs via the P_2 branch and its satellite, both having similar transition strength,⁶ then the two spin states will be equally populated by laser excitation. The other two possibilities for the pumping transition, however, favor collisional spin-state relaxation. Of these, the R_2 branch has no satellite and only one spin state can be pumped directly. As discussed earlier, it is most probable pumping

TABLE 1. ESTIMATES OF NCO A + X SYSTEM LINE POSITIONS
IN 4658 Å REGION^a

Transition Type	Known Position in (0,0 ⁰ ,0) + (0,0 ¹ ,0) (cm ⁻¹)	Estimated Position in (0,0 ⁰ ,0) + (1,0 ¹ ,0) (cm ⁻¹)
⁰ P ₁₂ 33	22679	21405
P ₂ + ^P Q ₁₂ 32	22705	21431
Q ₂ + ^Q R ₁₂ 31	22729	21455
R ₂ 30	22753	21479
P ₁ 32	22779	21505
Q ₁ + ^Q P ₂₁ 31	22804	21530
R ₁ + ^R Q ₂₁ 30	22829	21555
^S R ₂₁ 29	22852	21578

^aKnown line positions were obtained from Ref. 5 and 6. Estimated line positions were obtained by subtracting the measured X²_π (1,0¹,0) vibrational energy from the known positions as described in the text. The argon 4658 Å laser line corresponds to an energy of 21463 cm⁻¹.

occurs in the Q_2 branch where the strength of the main branch and satellite transitions differ by a factor of about 3. Therefore, the interpretation of spin-state relaxation is favored.

In scans of fluorescence from $A^2\Sigma^+(0,0^0,0)$, besides the bands in the 4400 Å and 4658 Å region, Bondybey and English¹⁰ also observed weaker emissions near 4485 Å and 4820 Å. These were attributed to emission to $X^2\Sigma^+(0,1^0,0)$ and $X^2\Pi(0,0^1,1)$, respectively. Corrections for detection system sensitivity vs wavelength were not made in their study nor in the present work, but the wavelength range scanned is small enough that the sensitivity is not expected to change drastically. (In particular, sensitivities for the PMT's used in the two studies change less than 15% over the region of interest.) In the earlier study¹⁰ an unknown gain change was made between 4400 and 4485 Å. We have measured the intensity ratio for emission to $X^2\Pi(0,0^1,0)$ and $X^2\Sigma^+(0,1^0,0)$. Combining this with the earlier ratios for the three hot band intensities leads to an estimate of the intensity ratio between the two strongest bands. The resulting intensity ratio for $X^2\Pi(0,0^0,0)$ to $X^2\Pi(1,0^1,0)$ is about 2.8 : 1.* Emission to $X^2\Pi(0,0^1,1)$ could not be found using the 1 m monochromator. This may be due to two factors. First, the emission may be too broad to be seen easily at high resolution. Second, the laser power and performance were deteriorating in the late part of this study when the most diligent attempts to find the band were made. However, a very weak and rather broad doublet was observed with the 25 cm monochromator - OMA system which could be attributed to this band. Though C_2 fluorescence interferes with exact measurements in the 4658 Å region, the intensity ratios for the three hot bands are at least in qualitative agreement with Ref. 10.

One fluorescence spectrum from those with broad spectral envelopes shown in Figure 4 was selected for further study. The fluorescence intensity from the 4765 Å pump line was the strongest, about 0.2 times that from the 4658 Å line. A spectrum at 0.60 Å FWHM resolution taken with the 1 m monochromator is shown in Figure 10. The spectrum is noisier than for that from 4658 Å (Figure 5) due to the lower signal intensity. Nonetheless, the same seven bandheads as seen with the 4658 Å laser line may still be readily identified. In addition, several other bandheads and/or peaks at shorter wavelengths are present in Figure 10. It is readily seen from Ref. 10 that these emissions do not arise from the $A^2\Sigma^+(0,0^0,0)$ level. They may arise from excitation to some high vibrational level followed by vibrational relaxation populating a number of lower levels. Alternatively, the laser line could excite high-lying rotational levels from several vibrational levels in the ground state. Thus, the excitation line could populate more than one vibrational level in the A state resulting in a rather complex spectrum. Or, some combination of these two effects may take place. If significant vibrational relaxation does occur, it would seem to indicate that H_2O , CO_2 , H_2

*In a private communication, V.E. Bondybey informed us that though exact information was lost, the approximate gain change should lead to an intensity ratio of about 2 or 3:1, in good agreement with our result. Approximate intensity ratios for the other two bands may be derived from the fluorescence scan in Ref. 10. The results are also in reasonable agreement with preliminary results of a more careful determination to appear in Ref. 12b.

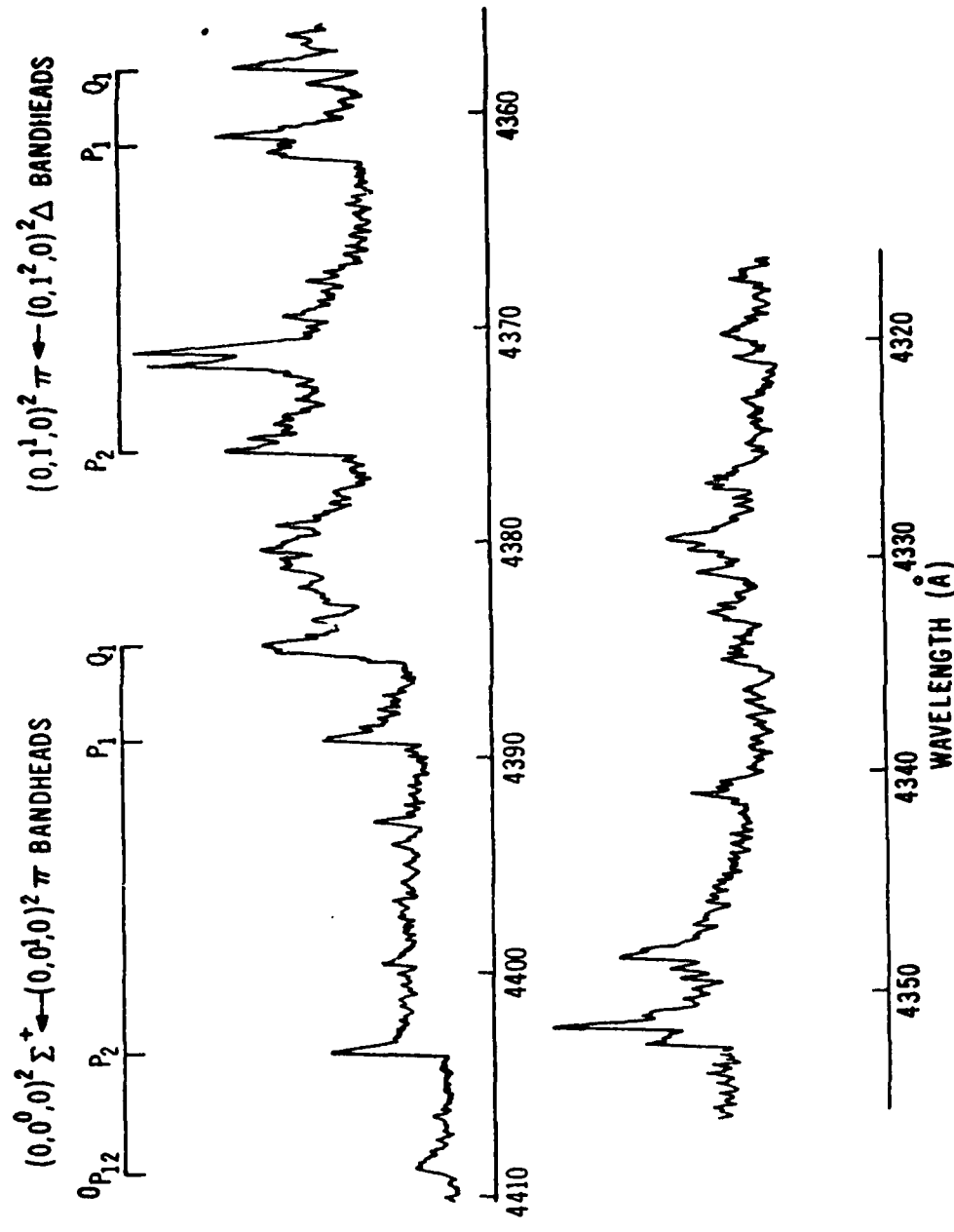


Figure 10. LEF Spectrum of NCO Using the 4765 Å Laser Line. The spectrum was taken at 0.60 Å FWHM resolution.

or CO (major species present under rich flame conditions) must be the collision partner since Sullivan et al¹² have found that vibrational relaxation of $A^2\Sigma^+$ NCO by N_2 and O_2 is very slow. The doublet observed at about 4371 Å in Figure 10 is rather intriguing. The sharpness of these peaks, similar in width to the prominent lines of Figure 5, suggests that perhaps one or both of them are due to emission from an initially pumped N' level. Higher resolution scans would be necessary to evaluate this possibility. We have not pursued this type of study at present.

B. NCO Density in the Flame

The NCO fluorescence may be readily used to map out relative densities in the flame. This was done using the 4658 Å excitation line since this excitation is the best understood. Also, the line excites the $A^2\Sigma^+$ (0,0⁰,0) level so that vibrational transfer to lower levels will not complicate data analysis. The technique is explained in this section.

Two basic assumptions must be made in order to make relative density measurements. First, one must assume the relative quenching rate is nearly constant throughout all positions of interest in the flame. At first glance, this assumption seems unreasonable for the flame front because the composition and temperature undergo drastic changes in that region. However, several recent studies indicate quenching rates are nearly constant in flame fronts, at least for OH.^{22,25,26} As will be seen shortly, the temperature is fairly constant over much of the region of interest. Also, one typically finds for premixed flames that the major species composition approximates that in the burnt gases very early in the flame front. Therefore the assumption of constant quenching rates is not unreasonable. The second basic assumption is that the X state of NCO is in thermal equilibrium at the flame temperature. One then calculates the relative density using the familiar Boltzmann equation. These assumptions lead to the very simple proportionality

$$n \propto FQ / (2J'' + 1) \exp(-E_{N'', J''} / kT) \quad (1)$$

where n is the density of NCO, F the fluorescence intensity, Q the molecular partition function, J'' is the angular momentum quantum number for the ground state and $E_{N'', J''}$ is the energy of the ground rotational state. For the present results we assumed the 4658 Å line pumps the $Q_2 31$ transition for which the ground state is $N'' = 31$, $J'' = 30.5$. However, even if the assignment of rotational branch for the pumping transition is incorrect, the factors in Eq. (1) still lead to the same relative density profiles. However, the estimate of absolute density, to appear later, would be affected. If the R_2 or P_2 transition is actually pumped at 4658 Å, our estimate of the rotational line strength is about a factor of 2 too high so that the calculated density would

²⁵J.H. Bechtel and R.F. Teets, "Hydroxyl and Its Concentration Profile in Methane-Air Flames," *Applied Opt.*, Vol. 18, p. 4138, 1979.

²⁶M.J. Cottureau and D. Stepowski, "Laser-Induced Fluorescence Spectroscopy Applied to the Hydroxyl Radical in Flames," *Laser Probes for Combustion Chemistry*, edited by D.R. Crosley, American Chemical Society Symposium Series 134, Washington, DC, p. 131, 1980.

be a corresponding factor too low. $E_{N^+,J}$ in Eq. (1) was estimated by using the measured^{9,10,12} $X^2\Pi(1,0^1,0)$ energy of 1274 cm^{-1} and assuming rotational constants are nearly equal in the $X^2\Pi(0,0^1,0)$ and $(1,0^1,0)$ states. The spin-orbit splitting^{5,6} of $\sim 98\text{ cm}^{-1}$ in $X^2\Pi$ was also considered.

The relative fluorescence intensity profiles were measured using the 25 cm monochromator - OMA system. The strong fluorescence for the entire band system between 4300 \AA and 4425 \AA was integrated to yield the intensities vs burner position. Temperature measurements were made using the spontaneous Raman signal from the Stokes rotational-vibrational Q-branch of N_2 . These Raman spectra were fitted using a multiparameter least squares computer program developed to extract temperature and N_2 concentration from the data. The standard deviation in flame temperatures is about 1%. The Raman methods are discussed in more detail in Ref. 13. The resulting temperature and relative density profiles are shown in Figure 11. The adiabatic flame temperature, calculated using the NASA-Lewis thermodynamic equilibrium code of Svehla and McBride,²⁷ is also indicated in the figure. Note that the measured peak temperature and adiabatic flame temperature are equal within experimental error, indicating minimal heat losses to the burner. The zero point on the relative position scale in Figure 11 corresponds to the top of the burner body. (See Figure 1.) The minimum distance between the top of the knife edges and the top of the burner body, where the measurements were taken, is $2.50 \pm 0.25\text{ mm}$. The steep concentration and temperature gradients at about $1.0 - 1.5\text{ mm}$ indicate the position of the leading edge of the flame reaction zone. Therefore, the reaction zone must extend about $1.0 - 1.5\text{ mm}$ below the top of the knife edges under our flow conditions. (This agrees reasonably well with a visual inspection of the luminous flame zone position.)

Besides the NCO and temperature profiles, relative $a^3\Pi_u C_2$ and $X^2\Pi CN$ profiles measured at the same time¹⁵ are shown for comparison in Figure 11. The density profiles are almost indistinguishable from the relative fluorescence intensity profiles (not shown), indicating the correction in Eq. (1) is small. It should be noted that the relative concentration profiles are only meaningful for individual compounds vs position; that is, the absolute peak concentrations of the three compounds are not accurately known. Figure 11 shows that the C_2 , CN and NCO concentrations all decay rapidly outside the reaction zone of the flame.

As discussed in Ref. 15, a very rough estimate of the absolute peak densities in Figure 11 may be made using three major assumptions. Briefly, one assumes: (1) The laser line is Doppler broadened at about room temperature.* (2) The molecular transition is Doppler broadened at the flame temperature of about 2500 K. (3) The quenching rate of excited molecular

²⁷R.A. Svehla and B.J. McBride, "Fortran IV Computer Program for Calculation of Thermodynamic and Transport Properties of Complex Chemical Systems," NASA TN D-7056, 1973 (1981 program version).

* Actually, the laser lineshape probably consists of about 20-30 cavity modes within the 0.04 cm^{-1} Doppler width.

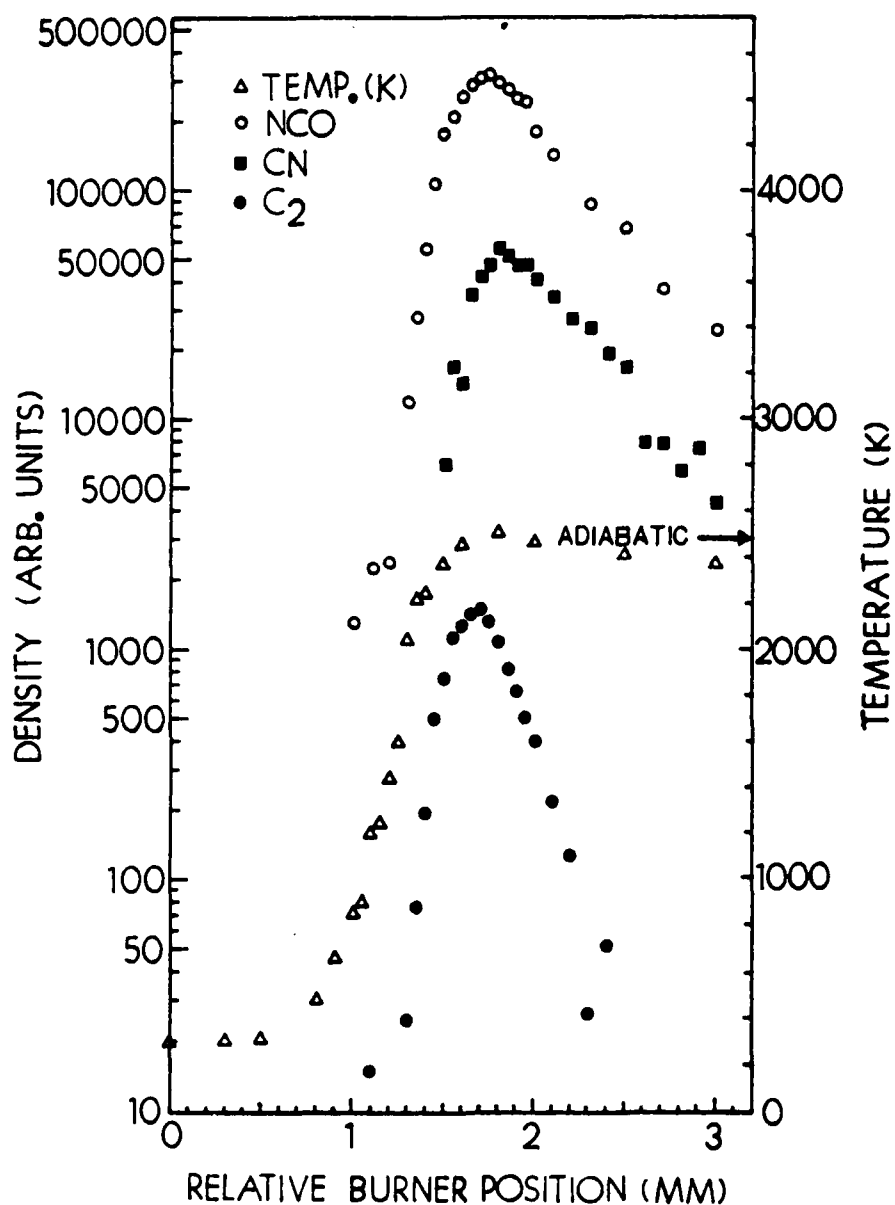


Figure 11. Measured Temperature and Relative Density Profiles of NCO, CN, and $a^3\Pi_u$ C₂ in a Slightly Rich CH₄/N₂O Flame. The calculated adiabatic flame temperature is also indicated. Relative densities may not be compared between compounds in this figure because curves for the individual compounds were only plotted with large separations for ease in visualization. Estimates of the absolute peak densities are given in the text.

species is about $1 \times 10^9 \text{ sec}^{-1}$, a typical value for atmospheric pressure flames.²⁸ Furthermore, measurements of NCO quenching rates by O_2 and N_2 ,¹² corrected to our temperature and pressure, indicate $1 \times 10^9 \text{ sec}^{-1}$ is a reasonable estimate to select. The calculation also requires some knowledge of the overlap of the laser pump line and the molecular transition. Data was available to estimate this quantity for C_2 and CN, but of course not for NCO since exact line positions are unknown. Therefore, the calculation for NCO assumed perfect overlap. Thus, only a lower limit for the density was computed. Finally, the fluorescence intensity was calibrated against the Raman N_2 signal from room air using the same laser lines as for fluorescence excitation. Calibration in this manner has two advantages in that it obviates the need for an absolute laser power or a sampling volume measurement. Using the estimated overlap for C_2 and CN leads to peak densities of $2 \times 10^{13} \text{ cm}^{-3}$ and $3 \times 10^{14} \text{ cm}^{-3}$, respectively.¹⁵ Spectroscopic data used for these estimates is discussed in Ref. 15. For NCO, the further necessary spectral data is the relative intensity of vibrational bands associated with $\text{A}^2\Sigma^+$ ($0,0^0,0$) and the radiative lifetime of this state. These may then be used to calculate Einstein coefficients. The estimated relative vibrational band intensities were obtained as discussed in the previous section. The fluorescence lifetime used was 400 nsec obtained from gas phase measurements.^{11,12} The lower limit for NCO density thus calculated is $3 \times 10^{14} \text{ cm}^{-3}$. Due to the various assumptions made in the absolute density calculations, it is difficult to place error limits on these quantities. The major source of random error in the calculated densities is in the spectral overlap because the densities are quite sensitive to these quantities. Of course, the lower limit for NCO does not depend on this quantity at all. Most probably the largest source of systematic error is in the assumed quenching rate of $1 \times 10^9 \text{ sec}^{-1}$ which is probably only good to within about a factor of five. The densities are therefore believed to be good to within factors of about 10 for CN, 20 for a $^3\Pi_u$ C_2 and 5 for the lower limit for NCO. These estimates should be useful in determining whether chemistry of these trace species must be considered in $\text{CH}_4/\text{N}_2\text{O}$ flame models.

Attempts were made to find C_2 , CN and NCO in a slightly rich CH_4/air flame (exact composition unknown). The sensitivity limits were for densities about a factor of 100 lower than in the $\text{CH}_4/\text{N}_2\text{O}$ flame. Fluorescence was found for C_2 , but not for CN or NCO. This result indicates a probable difference in the nitrogen chemistry for the two flames. Earlier studies of OH and, in particular, NH concentrations in the stoichiometric flames led to the same conclusion.²² This should not be extremely surprising because the N - N bond strength in N_2 is much stronger than in N_2O making N_2 more chemically inert. We have not attempted to analyze details of the chemistry at present.

IV. CONCLUSIONS

Laser excited fluorescence from the A - X system of NCO has been identified in a rich atmospheric pressure $\text{CH}_4/\text{N}_2\text{O}$ flame using an argon laser pump source. LEF was obtained for all nine available laser lines ranging from 4545 Å to 5145 Å. The hot flame source of NCO aids in the pumping scheme

²⁸A similar assumption is made in D.R. Crosley, "Collisional Effects on Laser-Induced Fluorescence Flame Measurements," *Opt. Eng.*, Vol. 20, p. 511, 1981.

since all of the available laser lines must pump vibrational hot bands of the NCO to the red of the main 4400 Å band. The 4658 Å laser line appears to be by far the most useful of the available lines for diagnostic purposes. This line pumps in the $A^2\Sigma^+ (0,0^0,0) + X^2\Pi (1,0^1,0)$ band. It appears that this is why the LEF is most intense for this pump line. NCO is pumped to the $N' = 31$ excited level by the 4658 Å line. However, the rotational branch of the pumping transition could not be firmly established. At present, the Q_231 appears to be the most likely candidate.

The 4658 Å pump line was used to measure accurate relative density profiles in the CH_4/N_2O flame. In addition, a lower limit for the absolute number density of $\sim 3 \times 10^{14} \text{ cm}^{-3}$ was estimated using the available spectroscopic data and an assumed quenching rate. The argon laser source has proven to be quite useful for flame measurements of NCO. It should thus be useful for other hot sources of NCO in which cw measurements are desired.

ACKNOWLEDGEMENTS

The authors gratefully acknowledge the help of Mr. Calvin E. Weaver in construction of detection system electronics. Also, we would like to thank Dr. Vladimir E. Bondyey for sending us copies of original spectral data used in Ref. 10.

REFERENCES

1. (a) G.B. Debrow, J.M. Goodings, and D.K. Bohme, "Flame-Ion Probe of Intermediates Leading to NO_x in $\text{CH}_4\text{-O}_2\text{-N}_2$ Flames," Combustion and Flame, Vol. 39, p. 1, 1980. (b) C. Morley, "The Mechanism of NO Formation from Nitrogen Compounds in Hydrogen Flames Studied by Laser Fluorescence," 18th Symposium (International) on Combustion, The Combustion Institute, Pittsburgh, PA, p. 23, 1981. (c) Y.H. Song, D.W. Blair, V.J. Siminski, and W. Bartok, *ibid*, "Conversion of Fixed Nitrogen to N_2 in Rich Combustion," p. 53; and references therein.
2. (a) R.A. Beyer, "Molecular Beam Sampling Mass Spectrometry of High Heating Rate Pyrolysis: Description of Data Acquisition System and Pyrolysis of HMX in a Polyurethane Binder," ARBRL-MR-02816, 1978 (AD A054328). (b) C.U. Morgan and R.A. Beyer, "ESR and IR Spectroscopic Studies of HMX and RDX Thermal Decomposition," 15th JANNAF Combustion Meeting, Newport, RI, September 1978.
3. R.A. Fifer and H.E. Holmes, "Kinetics of the $\text{HCN} + \text{NO}_2$ Reaction Behind Shock Waves," to appear in J. Phys. Chem..
4. R. Holland, D.W.G. Style, R.N. Dixon, and D.A. Ramsay, "Emission and Absorption Spectra of NCO and NCS," Nature, Vol. 182, p. 336, 1958.
5. R.N. Dixon, "The Absorption Spectrum of the Free NCO Radical," Phil. Trans. Roy. Soc., Vol. 252, p. 165, 1960.
6. P.S.H. Bolman, J.M. Brown, A. Carrington, I. Kopp, and D.A. Ramsay, "A Re-Investigation of the $\text{A}^2\Sigma^+ - \text{X}^2\Pi$ Band System of NCO," Proc. Roy. Soc., Vol. A343, p. 17, 1975.
7. R.N. Dixon, "A $2\Pi = 2\Pi$ Electronic Band System of the Free NCO Radical," Can. J. Phys., Vol. 38, p. 10, 1960.
8. H. Okabe, "Photodissociation of HNCO in the Vacuum Ultraviolet; Production of $\text{NCO } \text{A}^3\Pi$ and $\text{NH } (\text{A}^3\Pi, \text{c}^1\Pi)$," J. Chem. Phys., Vol. 53, p. 3507, 1970.
9. D.E. Milligan and M.E. Jacox, "Matrix Isolation Study of the Infrared and Ultraviolet Spectra of the Free Radical NCO," J. Chem. Phys., Vol. 47, p. 5157, 1967.
10. V.E. Bondybey and J.H. English, "Fermi Resonance and Vibrational Relaxation in the $\text{A}^2\Sigma$ State of NCO in Solid Argon," J. Chem. Phys., Vol. 67, p. 2868, 1977.
11. H. Reisler, M. Mangir, and C. Wittig, "The Kinetics of Free Radicals Generated by IR Laser Photolysis. II. Reactions of $\text{C}_2(\text{X}^1\Sigma^+)$, $\text{C}_2(\text{a}^3\Pi)$, $\text{C}_3(\text{X}^1\Sigma_g^+)$ and $\text{CN}(\text{X}^2\Sigma^+)$ with O_2 ," Chem. Phys., Vol. 47, p. 49, 1980.

12. (a) B.J. Sullivan, G.P. Smith, D.R. Crosley, and G. Black, "Laser-Induced Fluorescence Studies of the NCO Molecule," Eastern States Fall Technical Meeting of the Combustion Institute, Pittsburgh, PA, Paper 44, October 1981. (b) B.J. Sullivan, G.P. Smith, and D.R. Crosley, to be published.
13. J.A. Vanderhoff, R.A. Beyer, and A.J. Kotlar, "Laser Raman Spectroscopy of Flames; Temperature and Concentrations in CH₄/N₂O Flames," ARBRL-TR-02388, January 1982 (AD A112326).
14. J.A. Vanderhoff, R.A. Beyer, W.R. Anderson, and A.J. Kotlar, "Ar⁺ Laser Excited Fluorescence Profiles of Radicals Produced in a CH₄/N₂O Flame," 36th Symposium on Molecular Spectroscopy, Columbus, Ohio, June 1981.
15. J.A. Vanderhoff, R.A. Beyer, A.J. Kotlar, and W.R. Anderson, "Ar⁺ Laser Excited Fluorescence of C₂ and CN Produced in a Flame," to appear in Combustion and Flame.
16. W.R. Anderson, A.J. Kotlar and J.A. Vanderhoff, to be published.
17. W.R. Anderson, J.A. Vanderhoff, A.J. Kotlar, L.J. Decker, and R.A. Beyer, "Laser Excitation of NCO A - X System Fluorescence in a CH₄/N₂O Flame Using an Argon Ion Laser," Eastern States Fall Technical Meeting of the Combustion Institute, Pittsburgh, PA, Paper 47, October 1981.
18. R.A. Beyer and M.A. DeWilde, "Simple Burner for Laser Probing of Flames," Rev. Sci. Instrum., Vol. 53, p. 103, 1982.
19. C. Chan and J.W. Daily, "Laser Excitation Dynamics of OH in Flames," Applied Opt., Vol. 19, p. 1357, 1980.
20. G.P. Smith and D.R. Crosley, "Quantitative Laser-Induced Fluorescence in OH: Transition Probabilities and the Influence of Energy Transfer," 18th Symposium (International) on Combustion, The Combustion Institute, Pittsburgh, PA, p. 1511, 1981.
21. A.C. Eckbreth, P.A. Bonczyk, and J.F. Verdick, "Investigation of CARS and Laser-Induced Fluorescence for Practical Combustion Diagnosis," Report No. EPA - 600/7-80-091, May 1980. Example spectra abstracted from this report may be found in: A.C. Eckbreth, "Spatially Precise Laser Diagnostics for Practical Combustor Probing," Laser Probes for Combustion Chemistry, edited by D.R. Crosley, American Chemical Society Symposium Series 134, Washington, D.C., p. 271, 1980; J.F. Verdick and P.A. Bonczyk, "Laser-Induced Saturated Fluorescence Investigations of CH, CN and NO in Flames," 18th Symposium (International) on Combustion, The Combustion Institute, Pittsburgh, PA, p. 1559, 1981.
22. W.R. Anderson, L.J. Decker, and A.J. Kotlar, "Concentration Profiles of NH and OH in a Stoichiometric CH₄/N₂O Flame by Laser Excited Fluorescence and Absorption," to appear in Combustion and Flame.
23. Atomic line positions were obtained from G.R. Harrison, Massachusetts Institute of Technology Wavelength Tables, M.I.T. Press, Cambridge, MA, 1969.
24. C.E. Moore and H.P. Broida, "CH in the Solar Spectrum," J. Res. Nat. Bur. Stand., Vol. 63A, p. 19, 1959.

25. J.H. Bechtel and R.E. Teets, "Hydroxyl and Its Concentration Profile in Methane-Air Flames," Applied Opt., Vol. 18, p. 4138, 1979.
26. M.J. Cottreau and D. Stepowski, "Laser-Induced Fluorescence Spectroscopy Applied to the Hydroxyl Radical in Flames," Laser Probes for Combustion Chemistry, edited by D.R. Crosley, American Chemical Society Symposium Series 134, Washington, DC, p. 131, 1980.
27. R.A. Svehla and B.J. McBride, "Fortran IV Computer Program for Calculation of Thermodynamic and Transport Properties of Complex Chemical Systems," NASA TN D-7056, 1973 (1981 program version).
28. A similar assumption is made in D.R. Crosley, "Collisional Effects on Laser-Induced Fluorescence Flame Measurements," Opt. Eng., Vol. 20, p. 511, 1981.

DISTRIBUTION LIST

<u>No. Of Copies</u>	<u>Organization</u>	<u>No. Of Copies</u>	<u>Organization</u>
12	Administrator Defense Technical Info Center ATTN: DTIC-DDA Cameron Station Alexandria, VA 22314	4	Commander US Army Research Office ATTN: R. Girardelli D. Mann R. Singleton D. Squire Research Triangle Park, NC 27709
1	Commander USA DARCOM ATTN: DRCDMD-ST 5001 Eisenhower Avenue Alexandria, VA 22333	1	Commander USA Communications Research and Development Command ATTN: DRSEL-ATDD Fort Monmouth, NJ 07703
1	Commander USA ARRADCOM ATTN: DRDAR-TDC D. Gyrog Dover, NJ 07801	1	Commander USA Electronics Research and Development Command Technical Support Activity ATTN: DELSD-L Fort Monmouth, NJ 07703
2	Commander USA ARRADCOM ATTN: DRDAR-TSS Dover, NJ 07801	2	Commander USA ARRADCOM ATTN: DRDAR-LCA-G, D.S. Downs J.A. Lannon Dover, NJ 07801
1	Commander USA ARRCOM ATTN: DRSAR-LEP-L Rock Island, IL 61299	1	Commander USA ARRADCOM ATTN: DRDAR-LC, L. Harris Dover, NJ 07801
1	Director USA ARRADCOM Benet Weapons Laboratory ATTN: DRDAR-LCB-TL Watervliet, NY 12189	1	Commander USA ARRADCOM ATTN: DRDAR-SCA-T, L. Stiefel Dover, NJ 07801
1	Commander USA Aviation Research and Development Command ATTN: DRDAV-E 4300 Goodfellow Blvd. St. Louis, MO 63120	1	Commander USA Missile Command ATTN: DRSMI-R Redstone Arsenal, AL 35898
1	Director USA Air Mobility Research and Development Laboratory Ames Research Center Moffett Field, CA 94035	1	Commander USA Missile Command ATTN: DRSMI-YDL Redstone Arsenal, AL 35898

DISTRIBUTION LIST

<u>No. Of Copies</u>	<u>Organization</u>	<u>No. Of Copies</u>	<u>Organization</u>
1	Commander USA Missile Command ATTN: DRSMI-RK, D.J. Ifshin Redstone Arsenal, AL 35898	1	Commander Naval Surface Weapons Center ATTN: J.L. East, Jr., G-20 Dahlgren, VA 22448
1	Commander USA Tank Automotive Command ATTN: DRSTA-TSL Warren, MI 48090	1	Commander Naval Surface Weapons Center ATTN: G.B. Wilmot, R-16 Silver Spring, MD 20910
1	Director USA TRADOC Systems Analysis Activity ATTN: ATAA-SL WSMR, NM 88002	4	Commander Naval Weapons Center ATTN: R.L. Derr, Code 389 China Lake, CA 93555
2	Commandant US Army Infantry School ATTN: ATSH-CD-CSO-OR Fort Benning, FA 31905	1	Commander Naval Weapons Center ATTN: T. Boggs China Lake, CA 93555
1	Chief of Naval Research ATTN: R.S. Miller, Code 432 800 N. Quincy Street Arlington, VA 22217	1	Commander Naval Research Laboratory Washington, DC 20375
1	Navy Strategic Systems Project Office ATTN: R.D. Kinert, SP 2731 Washington, DC 20360	1	Commanding Officer Naval Underwater Systems Center Weapons Dept. ATTN: R.S. Lazar/Code 36301 Newport, RI 02840
1	Commander Naval Air Systems Command ATTN: J. Ramnarace, AIR-54111C Washington, DC 20360	1	Superintendent Naval Postgraduate School Dept. of Aeronautics ATTN: D.W. Netzer Monterey, CA 93940
3	Commander Naval Ordnance Station ATTN: C. Irish S. Mitchell P.L. Stang, Code 515 Indian Head, MD 20640	6	AFRPL (DRSC) ATTN: R. Geisler D. George B. Goshgarian J. Levine W. Roe D. Weaver Edwards AFB, CA 93523

DISTRIBUTION LIST

<u>No. Of Copies</u>	<u>Organization</u>	<u>No. Of Copies</u>	<u>Organization</u>
1	AFATL/DLDD ATTN: O.K. Heiney Eglin AFB, FL 32542	1	AVCO Corporation AVCO Everett Rsch. Lab. Div. ATTN: D. Stickler 2385 Revere Beach Parkway Everett, MA 02149
1	AFOSR ATTN: L.H. Caveny Bolling Air Force Base Washington, DC 20332	1	Battelle-Memorial Institute Tactical Technology Center ATTN: J. Huggins 505 King Avenue Columbus, OH 43201
1	AFWL/SUL Kirtland AFB, NM 87117		
1	NASA Langley Research Center ATTN: G.B. Northam/MS 168 Hampton, VA 23365	2	Exxon Research & Engineering ATTN: A. Dean M. Chou P.O. Box 45 Linden, NJ 07036
4	National Bureau of Standards ATTN: J. Hastie M. Jacox T. Kashiwagi H. Semerjian Washington, DC 20234	1	Ford Aerospace and Communications Corp. DIVAD Division Div. Hq., Irvine ATTN: D. Williams Main Street & Ford Road Newport Beach, CA 92663
1	Aerojet Solid Propulsion Co. ATTN: P. Micheli Sacramento, CA 95813	1	General Electric Armament & Electrical Systems ATTN: M.J. Bulman Lakeside Avenue Burlington, VT 05402
1	Applied Combustion Technology, Inc. ATTN: A.M. Varney P.O. Box 17885 Orlando, FL 32860	1	General Electric Company ATTN: M. Lapp Schenectady, NY 12301
2	Atlantic Research Corp. ATTN: M.K. King 5390 Cherokee Avenue Alexandria, VA 22314	1	General Electric Ordnance Systems ATTN: J. Landzy 100 Plastic Avenue Pittsfield, MA 01203
1	Atlantic Research Corp. ATTN: R.H.W. Waesche 7511 Wellington Road Gainesville, VA 22065	1	General Motors Rsch Labs Physics Department ATTN: J.H. Bechtel Warren, MI 48090

DISTRIBUTION LIST

<u>No. Of Copies</u>	<u>Organization</u>	<u>No. Of Copies</u>	<u>Organization</u>
3	Hercules, Inc. Alleghany Ballistics Lab. ATTN: R.R. Miller P.O. Box 210 Cumberland, MD 21501	1	Science Applications, Inc. ATTN: H. S. Pergament 1100 State Rd., Bldg. N Princeton, NJ 08540
3	Hercules, Inc. Bacchus Works ATTN: K.P. McCarty P.O. Box 98 Magna, UT 84044	1	Olin Corporation Smokeless Powder Operations ATTN: R.L. Cook P.O. Box 222 St. Marks, FL 32355
1	Hercules, Inc. AFATL/DLDD ATTN: R.L. Simmons Eglin AFB, FL 32542	1	Paul Gough Associates, Inc. ATTN: P.S. Gough 1048 South Street Portsmouth, NH 03801
1	Honeywell, Inc. Defense Systems Division ATTN: D.E. Broden/ MS MN50-2000 600 2nd Street NE Hopkins, MN 55343	2	Princeton Combustion Research Laboratories ATTN: M. Summerfield N.A. Messina 1041 US Highway One North Princeton, NJ 08540
1	IBM Corporation ATTN: A.C. Tam Research Division 5600 Cottle Road San Jose, CA 95193	1	Pulsepower Systems, Inc. ATTN: L.C. Elmore 815 American Street San Carlos, CA 94070
1	Director Lawrence Livermore P.O. Box 808 ATTN: C. Westbrook Livermore, CA 94550	1	Rockwell International Corp. Rocketdyne Division ATTN: J.E. Flanagan/HB02 6633 Canoga Avenue Canoga Park, CA 91304
1	Lockheed Palo Alto Rsch Lab ATTN: George Lo 3251 Hanover Street Dept. 52-35/B204/2 Palo Alto, CA 94304	2	Sandia National Laboratories Combustion Sciences Dept. ATTN: R. Cattolica D. Stephenson Livermore, CA 94550
1	Los Alamos National Lab T7, MS-B284 P.O. Box 1663 Los Alamos, NM 87545	1	Science Applications, Inc. ATTN: R.B. Edelman 23146 Cumorah Crest Woodland Hills, CA 91364

DISTRIBUTION LIST

<u>No. Of Copies</u>	<u>Organization</u>	<u>No. Of Copies</u>	<u>Organization</u>
1	United Technologies ATTN: A. C. Eckbreth East Hartford, CT 06108	2	United Technologies Corp. ATTN: R.S. Brown R.O. McLaren P.O. Box 358 Sunnyvale, CA 94086
1	Space Sciences, Inc. ATTN: M. Farber Monrovia, CA 91016	1	Universal Propulsion Company ATTN: H.J. McSpadden Black Canyon Stage 1 Box 1140 Phoenix, AZ 85029
4	SRI International ATTN: S. Barker D. Crosley D. Golden Tech Lib 333 Ravenswood Avenue Menlo Park, CA 94025	1	Veritay Technology, Inc. ATTN: E.B. Fisher P.O. Box 22 Bowmansville, NY 14026
1	Stevens Institute of Tech. Davidson Laboratory ATTN: R. McAlevy, III Hoboken, NJ 07030	1	Brigham Young University Dept. of Chemical Engineering ATTN: M.W. Beckstead Provo, UT 84601
1	Teledyne McCormack-Selph ATTN: C. Leveritt 3601 Union Road Hollister, CA 95023	1	California Institute of Technology Jet Propulsion Laboratory MS 125/159 4800 Oak Grove Drive Pasadena, CA 91103
1	Thiokol Corporation Elkton Division ATTN: W.N. Brundige P.O. Box 241 Elkton, MD 21921	1	California Institute of Technology ATTN: F.E.C. Culick/ MC 301-46 204 Karman Lab. Pasadena, CA 91125
3	Thiokol Corporation Huntsville Division ATTN: D.A. Flanagan Huntsville, AL 35807	1	University of California, Berkeley Mechanical Engineering Dept. ATTN: J. Daily Berkeley, CA 94720
3	Thiokol Corporation Wasatch Division ATTN: J.A. Peterson P.O. Box 524 Brigham City, UT 84302	1	University of California Los Alamos National Lab. ATTN: T.D. Butler P.O. Box 1663, Mail Stop B216 Los Alamos, NM 87545

DISTRIBUTION LIST

<u>No. Of Copies</u>	<u>Organization</u>	<u>No. Of Copies</u>	<u>Organization</u>
2	University of California, Santa Barbara Quantum Institute ATTN: K. Schofield M. Steinberg Santa Barbara, CA 93106	1	Hughes Aircraft Company ATTN: T.E. Ward 8433 Fallbrook Avenue Canoga Park, CA 91304
1	University of Southern California Dept. of Chemistry ATTN: S. Benson Los Angeles, CA 90007	1	University of Illinois Dept of Mech Eng ATTN: H. Krier 144 MED, 1206 W. Green Street Urbana, IL 61801
1	Case Western Reserve Univ. Div. of Aerospace Sciences ATTN: J. Tien Cleveland, OH 44135	1	Johns Hopkins University/APL Chemical Propulsion Information Agency ATTN: T.W. Christian Johns Hopkins Road Laurel, MD 20707
1	Cornell University Department of Chemistry ATTN: E. Grant Baker Laboratory Ithaca, NY 14853	1	University of Minnesota Dept. of Mechanical Engineering ATTN: E. Fletcher Minneapolis, MN 55455
1	Univ. of Dayton Rsch Inst. ATTN: D. Campbell AFRPL/PAP Stop 24 Edwards AFB, CA 93523	1	University of North Carolina at Chapel Hill Department of Chemistry ATTN: G. Hills Venable Hall 045A Chapel Hill, NC 27514
1	University of Florida Dept. of Chemistry ATTN: J. Winefordner Gainesville, FL 32601	4	Pennsylvania State University Applied Research Laboratory ATTN: G.M. Faeth K.K. Kuo H. Palmer M. Micci University Park, PA 16802
3	Georgia Institute of Technology School of Aerospace Engineering ATTN: E. Price Atlanta, GA 30332	1	Polytechnic Institute of NY ATTN: S. Lederman Route 110 Farmingdale, NY 11735
2	Georgia Institute of Technology School of Aerospace Engineering ATTN: W.C. Strahle B.T. Zinn Atlanta, GA 30332		

DISTRIBUTION LIST

<u>No. Of Copies</u>	<u>Organization</u>	<u>No. Of Copies</u>	<u>Organization</u>
2	Princeton University Forrestal Campus Library ATTN: K. Brezinsky I. Glassman P.O. Box 710 Princeton, NJ 08540	1	Stanford University Dept. of Mechanical Engineering ATTN: R. Hanson Stanford, CA 94305
1	Princeton University MAE Dept. ATTN: F.A. Williams Princeton, NJ 08544	2	University of Texas Dept. of Chemistry ATTN: W. Gardiner H. Schaefer Austin, TX 78712
2	Purdue University School of Aeronautics and Astronautics ATTN: R. Glick J.R. Osborn Grissom Hall West Lafayette, IN 47907	1	University of Utah Dept. of Chemical Engineering ATTN: G. Flandro Salt Lake City, UT 84112
3	Purdue University School of Mechanical Engineering ATTN: N.M. Laurendeau S.N.B. Murthy D. Sweeney TSPC Chaffee Hall West Lafayette, IN 47906	1	Virginia Polytechnical Institute and State University ATTN: J.A. Schetz Blacksburg, VA 24061
1	Rensselaer Polytechnic Inst. Dept. of Chemical Engineering ATTN: A. Fontijn Troy, NY 12181		<u>Aberdeen Proving Ground</u> Dir, USAMSAA ATTN: DRXSY-D DRXSY-MP, H. Cohen Cdr, USATECOM ATTN: DRSTE-TO-F Dir, USACSL, Bldg. E3516, EA ATTN: DRDAR-CLB-PA DRDAR-CLN DRDAR-CLJ-L
2	Southwest Research Institute ATTN: Robert E. White A.B. Wenzel 8500 Culebra Rd. San Antonio, TX 78228		

USER EVALUATION OF REPORT

Please take a few minutes to answer the questions below; tear out this sheet, fold as indicated, staple or tape closed, and place in the mail. Your comments will provide us with information for improving future reports.

1. BRL Report Number _____

2. Does this report satisfy a need? (Comment on purpose, related project, or other area of interest for which report will be used.)

3. How, specifically, is the report being used? (Information source, design data or procedure, management procedure, source of ideas, etc.) _____

4. Has the information in this report led to any quantitative savings as far as man-hours/contract dollars saved, operating costs avoided, efficiencies achieved, etc.? If so, please elaborate.

5. General Comments (Indicate what you think should be changed to make this report and future reports of this type more responsive to your needs, more usable, improve readability, etc.) _____

6. If you would like to be contacted by the personnel who prepared this report to raise specific questions or discuss the topic, please fill in the following information.

Name: _____

Telephone Number: _____

Organization Address: _____

FOLD HERE

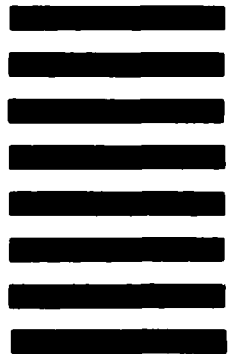
Director
US Army Ballistic Research Laboratory
ATTN: DRDAR-BLA-S
Aberdeen Proving Ground, MD 21005



NO POSTAGE
NECESSARY
IF MAILED
IN THE
UNITED STATES

OFFICIAL BUSINESS
PENALTY FOR PRIVATE USE, \$300

BUSINESS REPLY MAIL
FIRST CLASS PERMIT NO 12062 WASHINGTON, DC
POSTAGE WILL BE PAID BY DEPARTMENT OF THE ARMY



Director
US Army Ballistic Research Laboratory
ATTN: DRDAR-BLA-S
Aberdeen Proving Ground, MD 21005

FOLD HERE

END

FILMED

12-83

DTIC